analysis revealed that the increase was 38 ± 12% (BDNF-treated/BDNF-untreated; 1.38 ± 0.12; $p < 0.03$; $n = 4$ independent experiments). To exclude that the prosurvival effect of BDNF was the cause of the increase in neuronal cholesterol content, we counted the number of MAP-2-positive neurons in cultures incubated in the presence or absence of BDNF (200 ng/ml; 3 d). Quantitative analysis revealed that there was no significant difference in the number of neurons in these cultures (BDNF-treated/BDNF-untreated; 0.98 ± 0.07; $p < 0.03$).

To examine additionally whether BDNF stimulated cholesterol synthesis per se, we sought to normalize cholesterol content to the protein content of the cultures. In contrast to the number of MAP-2-positive neurons, the total protein content was increased significantly by 16 ± 3% ($p < 0.03$) in BDNF-treated cultures (200 ng/ml; 3 d). This is consistent with a previous report that BDNF elicits *de novo* protein synthesis in neurons (Takei et al., 2001). Even after normalization (cholesterol/total protein) BDNF significantly increased the cholesterol content (11 ± 4%; $p < 0.05$). Because the rise of cholesterol before normalization showed a pattern similar to that after this assessment, we have shown the cholesterol content in all experiments, because we confirmed that the number of MAP-2-positive neurons was not changed by treatment with the indicated drugs.

Together, these results suggest that BDNF elicits cholesterol biosynthesis in CNS neurons.

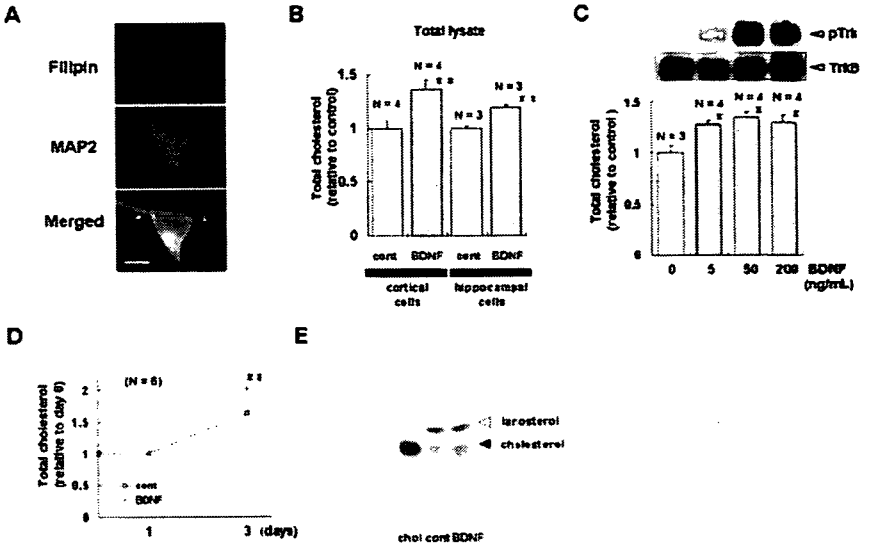

Figure 1. BDNF elicits cholesterol biosynthesis in cultured cortical and hippocampal neurons. Cholesterol content of cortical and hippocampal cells cultured under various conditions was measured. ***A***, Cholesterol in cultured cortical neurons was shown by staining cells with filipin, as described previously (Ma et al., 2003). Scale bar, 10 μm. ***B***, Cortical and hippocampal cells were cultured in the presence or absence of 200 ng/ml BDNF for 3 and 5 d, respectively. Compared with untreated cells (cont), BDNF-treated cortical and hippocampal cells had higher cholesterol contents. ***C***, BDNF increased the cholesterol content in cortical cells in a dose-dependent manner. Top, The TrkB receptor was activated by BDNF in a dose-dependent manner. Cell lysates were collected before or 3 min after treatment with the indicated concentration of BDNF. Immunoblotting was performed with anti-TrkB and anti-phospho-Trk antibodies, as described previously (Suzuki et al., 2004). Bottom, BDNF increased cholesterol content in a concentration-dependent manner. Cholesterol content was measured 3 d after treatment with the indicated concentration of BDNF. ***D***, A time course study of the BDNF-dependent cholesterol increase in cortical cells. Cells were cultured in the presence or absence of BDNF (200 ng/ml) for the indicated times, and the cholesterol amount was determined. ***E***, TLC analysis of cholesterol in BDNF-treated cortical neurons. Sterols were isolated from cortical neurons cultured in the presence or absence of BDNF (200 ng/ml) for 5 d. Extracts were dissolved in isopropyl alcohol and separated by TLC. Spots were visualized by using *p*-anisaldehyde. The positions of cholesterol and lanosterol are indicated with arrowheads. As a control, commercially obtained, purified cholesterol (chol) was loaded. Densitometric analysis demonstrated that the increase in cholesterol content in response to BDNF was 38 ± 12%. The value for each cholesterol band was normalized to that of the control sample. This and all other figures demonstrate that results are relative to control and are shown as the means ± SEM. Asterisks indicate a significant difference from control samples (Student's *t* test; $*p < 0.03$; $**p < 0.01$).

Involvement of TrkB activation in BDNF-induced cholesterol biosynthesis

Binding of BDNF to the TrkB receptor induces tyrosine autophosphorylation and activation of the receptor (Reichardt, 2006). To investigate whether TrkB activation was required for BDNF-mediated increases in cholesterol, we applied a general inhibitor of Trk tyrosine kinase, K252a (200 nM), to BDNF-treated (200 ng/ml) cortical cultures for 3 d. As reported previously (Tapley et al., 1992), K252a completely inhibited BDNF-induced TrkB phosphorylation (Fig. 2*A*, top). We found that K252a prevented the BDNF-induced increase in cholesterol content (Fig. 2*A*, bottom, BDNF plus K252a). This result suggests that TrkB activation is involved in BDNF-induced cholesterol biosynthesis. In addition, K252a treatment, which inhibited endogenous activation of the TrkB receptor (Fig. 2*A*, top), did not change the basal cholesterol content of the culture (Fig. 2*A*, bottom), indicating that endogenous BDNF is insufficient to stimulate cholesterol biosynthesis in these cultures.

BDNF-induced cholesterol biosynthesis is prevented by specific inhibitors of cholesterol synthesis pathway

Mevastatin is a specific inhibitor of HMG-CoA reductase, which converts HMG-CoA to mevalonate (Goldstein et al., 2006) (see Fig. 4*A*, HMGCR). Mevastatin treatment reduces the cholesterol level in cultured cortical neurons (Suzuki et al., 2004). We thus tested whether mevastatin also inhibited BDNF-induced increase of cholesterol content in cultured cortical cells. Treatment of the cells with 10 μM mevastatin (statin) for 3 d completely prevented the BDNF-mediated increase in cholesterol (Fig. 2*B*, BDNF plus statin). Importantly, this inhibition was restored by the addition of mevalonate, the product of the HMG-CoA reductase reaction; cholesterol levels were equivalent to those of cultures treated with BDNF alone (Fig. 2*B*, BDNF plus statin plus mevalonate).

We additionally examined the effect of zaragozic acid, a specific inhibitor of squalene synthase (see Fig. 4*A*, SQS) (Bergstrom et al., 1993), on the BDNF-induced increase in cholesterol. Treatment with zaragozic acid (100 μM; 3 d) completely blocked the BDNF effect (Fig. 2*C*, BDNF plus zaragozic acid). The inhibitory effect of zaragozic acid appeared to be comparable to that of mevastatin (Fig. 2*B*,*C*), supporting the hypothesis that BDNF stimulates the cholesterol synthesis pathway.

BDNF elicits cholesterol biosynthesis in neurons, but not in glial cells

Cholesterol biosynthesis occurs in both neurons and glial cells (Vance et al., 2005). Because BDNF raised the cholesterol content in cortical cell cultures (Fig. 1) containing a mixture of different cell types, we examined whether or not the BDNF-induced increase in cholesterol content was specific to neurons or glial cells.

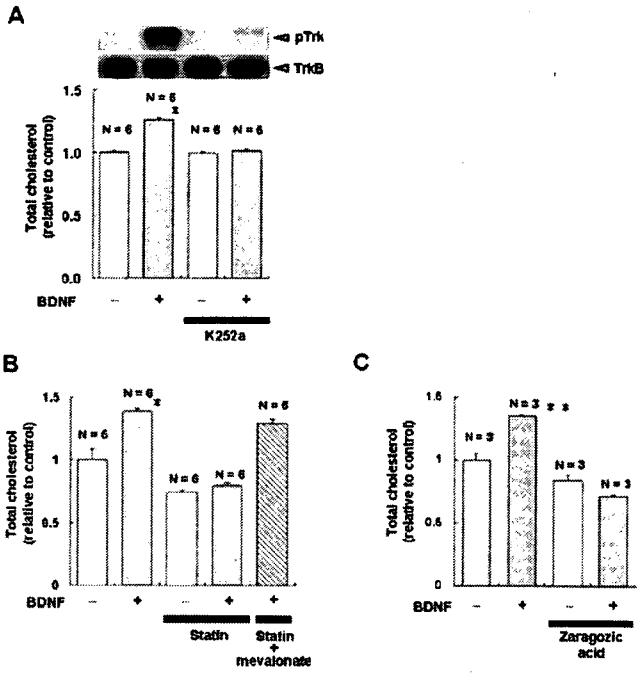

Figure 2. K252a, mevastatin, and zaragozic acid block BDNF-induced cholesterol biosynthesis in cortical neurons. Cholesterol content was measured 3 d after treatment with the indicated drugs. ***A***, Cultured cortical neurons were preincubated with or without 200 nM K252a for 1 h and then incubated with or without 200 ng/ml BDNF for 3 d. Top, The inhibitory effect of K252a on BDNF-induced activation of TrkB was investigated as described in Figure 1*C*. Cell lysates were collected before or 3 min after treatment with the indicated concentration of BDNF. Bottom, Cholesterol measurements. ***B***, ***C***, For the quantification of cholesterol content the cells were treated with the indicated reagents for 0 or 3 d in the presence or absence of 10 μM mevastatin (Statin; ***B***) and 100 μM zaragozic acid (***C***). Asterisks indicate a statistically significant difference from control group (Student's *t* test; $^{*}p < 0.001$; $^{**}p < 0.003$).

Neuron-rich cultures treated with Ara-C, which suppresses the growth of proliferative cells such as astrocytes (Ohira et al., 2005), were incubated in the presence or absence of BDNF (200 ng/ml; 3 d). The Ara-C-treated cultures had a 1.4 ± 0.21-fold higher neuronal population than the primary cultures in Figure 1 (Fig. 3*A*) (MAP-2-positive neurons, 91.2 ± 0.7%; GFAP-positive astrocytes, 5.4 ± 0.5%; O4-positive oligodendrocytes, 0.2 ± 0.2%; others, 5.2 ± 2.7%; $n = 3$ independent culture dishes). In these neuron-rich cultures the cholesterol content was increased significantly in response to BDNF (Fig. 3*A*) (1.34 ± 0.01-fold compared with control cultures). In primary cultures of astrocytes, however, BDNF treatment (200 ng/ml; 3 d) did not stimulate cholesterol biosynthesis (Fig. 3*C*), suggesting that BDNF does not promote cholesterol biosynthesis in glial cells. To test the possibility that neurons might be needed to increase the cholesterol content of glial cells in response to BDNF, we studied the expression of the full-length TrkB receptor (TrkB-FL) in glial cells and neurons in mixed cultures of these two cell types. In agreement with previous reports (Rose et al., 2003; Ohira et al., 2005), immunocytochemistry that used an antibody specific for TrkB-FL (Rasika et al., 1999) demonstrated that TrkB-FL signals were detectable only in MAP-2-positive neurons. No signals were detected in glial cells, even when they were cultured together with MAP-2-positive neurons (data not shown). Together with an earlier result showing that TrkB-FL activation is involved in BDNF-elicited cholesterol biosynthesis under mixed culture conditions (Fig. 2*A*), this result suggests that TrkB-FL-mediated BDNF signaling promotes cholesterol biosynthesis in neurons rather than in glial cells.

BDNF activates the transcription of cholesterol biosynthesis enzymes

To identify the mechanism by which BDNF elicits cholesterol biosynthesis, we examined whether BDNF stimulation upregulates the transcription of cholesterol biosynthesis enzymes, because previous work has shown that activation of cholesterol biosynthesis is accompanied by transcriptional control of these enzymes (Shimano, 2001). In this study we used quantitative reverse transcriptase-PCR to quantify the mRNA levels of several cholesterol biosynthesis enzymes. To exclude indirect effects of serum on the activity of genes involved in cholesterol biosynthesis, we cultured neurons in Neurobasal medium minus B27 supplement for 1 d before adding BDNF. HMG-CoA reductase is the first committed enzyme in the mevalonate pathway (Fig. 4*A*) (Goldstein et al., 2006). BDNF stimulation of neuron-rich cultures increased the mRNA for HMG-CoA reductase (HMGCR) by 88 ± 6% (Fig. 4*B*) ($n = 3$ independent culture dishes) within 1 h of stimulation, and this increase continued for 24 h (Fig. 4*B*, HMGCR) ($p < 0.01$). BDNF also increased the mRNA for mevalonate pyrophosphate decarboxylase (MPD), which converts mevalonate pyrophosphate into isopentenyl pyrophosphate (Fig. 4*B*, MPD) ($p < 0.03$), with a time course similar to that of HMGCR. We additionally studied the expression of mRNA for SQS, which catalyzes the first specific step in the cholesterol biosynthetic pathway, and SREBP-2, which is a transcription factor regulating the expression of cholesterol biosynthesis enzymes (Brown and Goldstein, 1999) (Fig. 4*B*, SQS and SREBP-2). Neither SQS nor SREBP-2 mRNA significantly increased up to 24 h after BDNF treatment ($p > 0.05$). In contrast, cultured astrocytes did not increase significantly the mRNA levels of any of these enzymes either at 1 or 24 h after BDNF application (Fig. 4*C*). These results therefore suggest that BDNF induces the expression of mRNA for cholesterol biosynthesis enzymes in neurons, but not in glial cells, and that the BDNF-stimulated increase in cholesterol content might be controlled at the transcriptional level.

BDNF increases the amount of cholesterol and caveolin-2 in neuronal lipid rafts

Because lipid rafts are cholesterol-rich microdomains (Simons and Toomre, 2000), we examined whether the cholesterol synthesized in response to BDNF accumulates in raft domains. Lipid raft fractions can be isolated by using the detergent-insoluble property of cholesterol (Simons and Toomre, 2000). We prepared lipid raft fractions from cultured cortical neurons, using our previously reported method (Suzuki et al., 2004). In this preparation cholesterol and the lipid raft marker caveolin-2 were enriched in fraction 2, and a nonraft membrane marker, the transferrin receptor (TfR), was enriched in fraction 6 (Fig. 5*A*). We compared the cholesterol content in the lipid raft fraction and the nonraft fraction between control and BDNF-treated cultures. BDNF treatment (200 ng/ml; 3 d) led to a robust increase in cholesterol in the lipid raft fraction, but not in the nonraft fraction (Fig. 5*B*, top panels) (fraction 2_{+BDNF}, 1.55 ± 0.02-fold; fraction 6_{+BDNF}, ND). The increase in cholesterol in the lipid raft fraction was similar to the extent of cholesterol increase in total lysates [compare Figs. 5*B* (top panels, 1.55 ± 0.02-fold) and 1*B* (1.36 ± 0.10-fold)], suggesting that the cholesterol produced in response to BDNF stimulation is a predominant feature of neuronal lipid rafts. In our earlier study the normalization of cholesterol to total protein indicated that BDNF stimulated cholesterol synthesis per se. We therefore sought to normalize cholesterol to the protein content of lipid raft fraction and nonraft fraction. We found that BDNF elicited an increase in protein content in the

nonraft fraction, but not in the raft fraction (Fig. 5*B*, bottom panels) (nonrafts, 1.49 ± 0.02-fold; $p < 0.001$) and the cholesterol/protein ratio increased in the lipid raft fraction (BDNF-treated/BDNF-untreated; 1.35 ± 0.02; $p < 0.001$). Together, these results suggest that lipid rafts may play a structural role in BDNF-dependent cholesterol biosynthesis.

Given that cholesterol is a major component of rafts (Simons and Toomre, 2000), it would be of interest to determine whether BDNF promotes the development of these microdomains, and we therefore examined whether BDNF increased the amount of caveolin-2. Remarkably, BDNF treatment (200 ng/ml; 3 d) robustly increased the level of caveolin-2 in the raft fraction, whereas caveolin-2 was completely absent from the nonraft fractions of BDNF-treated cultures (Fig. 5*B*, middle panels). We also examined the effect of BDNF on the level of a nonraft marker protein, TfR. This protein did not show any changes in response to BDNF treatment (Fig. 5*B*, middle panels). Together, these results suggest that BDNF promotes the development of lipid rafts in CNS neurons by increasing their cholesterol content, which is required for the organization of this raft domain.

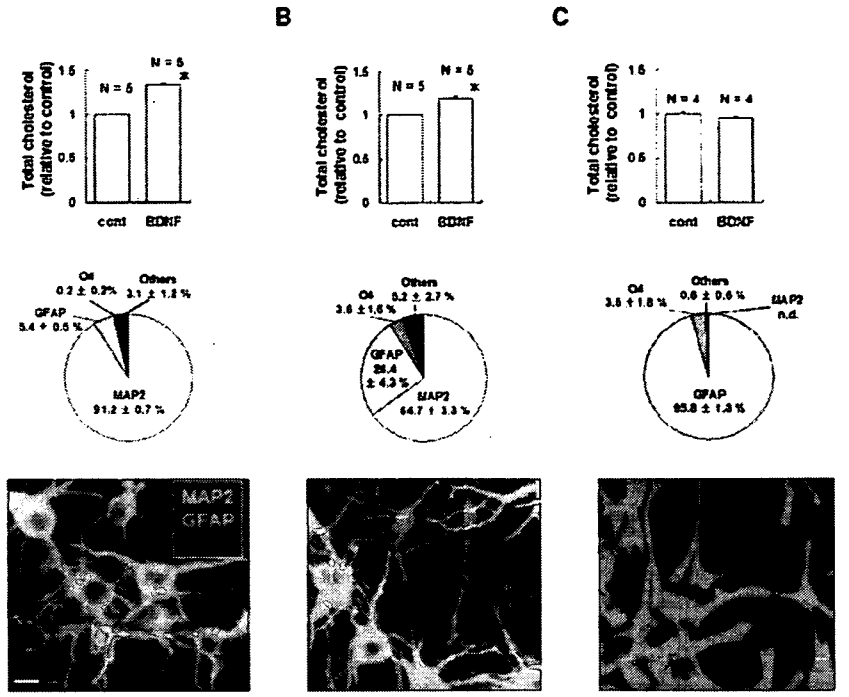

Figure 3. BDNF elicits cholesterol biosynthesis in neurons, but not in glial cells. *A*, *B*, Cortical cells were cultured in the presence or absence of BDNF (200 ng/ml; 3 d) and in the presence (*A*) or absence (*B*) of 1 μM Ara-C. *C*, Astrocyte cultures were treated with BDNF (200 ng/ml; 3 d). Cholesterol content (top) was determined. Cell type and fraction of the population (middle and bottom) were determined by immunocytochemistry, using antibodies against MAP-2, O4, and GFAP to identify neurons, oligodendrocytes, and glial cells, respectively. DAPI staining was performed to determine the number of living cells in culture. Note that neuron-rich cultures (*A*) showed the greatest increase in cholesterol in response to BDNF and that cultured astrocytes (*C*) did not show a significant increase in cholesterol content in response to BDNF. The asterisks indicate a statistically significant difference between control and BDNF samples (Student's *t* test; $^*p < 0.001$). Scale bar, 10 μm.

BDNF stimulates the increase and accumulation of presynaptic proteins in lipid rafts

Lipid rafts mediate BDNF signaling in dendritic growth (Suzuki et al., 2004). Herein we have clarified the role of lipid rafts on long-term regulation of synaptic development by BDNF. Treatment with BDNF for 2–3 d exerts the following pleiotropic effects: (1) continuous increase in quantal size as well as impulse-evoked synaptic transmission (Wang et al., 1995) and (2) increase in the number of docked vesicles and the number of presynaptic proteins (Takei et al., 1997; Tartaglia et al., 2001). Consistent with these reports, application of BDNF (200 ng/ml) for 3 d led to a significant increase in the number of puncta containing the presynaptic protein synaptophysin (Fig. 6*A*,*C*) (2.6 ± 0.4-fold increase relative to control cultures; $n = 8$ from two independent cultures; $p < 0.01$).

To understand the role of lipid rafts in BDNF-induced synapse development, we examined the number of presynaptic proteins in the lipid raft and nonraft fractions in BDNF-treated cortical neurons (200 ng/ml; 3 d). Remarkably, BDNF treatment resulted in a striking increase in the number of presynaptic proteins in lipid rafts (Fig. 6*B*). However, BDNF did not affect the numbers of these presynaptic proteins in the nonraft fraction. These results suggest that the BDNF-induced increase in presynaptic proteins during synapse development is associated specifically with the lipid raft microdomains.

This finding was supported by the following experiments. First, we examined the effect of a lipid raft disrupter mevastatin on the BDNF-induced increase in the number of synaptophysin-positive presynaptic puncta. Quantitative assessment demonstrated that mevastatin suppressed the BDNF increase in the number of synaptophysin-labeled puncta (Fig. 6*C*) (BDNF plus statin, 1.0 ± 0.2-fold). Neurons treated with mevastatin alone showed no significant change in the number of the puncta (Fig. 6*C*) (−BDNF plus statin, 0.58 ± 0.1-fold; $p > 0.08$). Quantitative analysis of soma size revealed that neither BDNF nor mevastatin affected the average soma size of MAP-2-positive neurons (data not shown), suggesting that BDNF promotes the development of the synapse, but not the cell body, via the stimulation of cholesterol synthesis.

Second, consistent with previous reports (Takei et al., 1997; Tartaglia et al., 2001), BDNF (200 ng/ml; 3 d) increased the amount of presynaptic protein (Fig. 6*B*, BDNF). This effect of BDNF, however, was prevented by mevastatin and zaragozic acid (Fig. 6*D*, BDNF plus statin; *E*, BDNF plus zaragozic acid). The amount of the neuronal marker protein class III tubulin (TUJ1) was not affected by these inhibitors. Moreover, zaragozic acid and mevastatin similarly inhibited the BDNF-induced increase in cholesterol, additionally supporting the hypothesis that BDNF-dependent cholesterol synthesis is crucial for synapse development.

Third, we previously showed that lipid rafts exhibited a gradual increase in the amount of BDNF and TrkB during development and that the amount of lipid raft-specific components, such as cholesterol and caveolin-2, increased during postnatal stages of development (Suzuki et al., 2004). Here we investigated the distribution of presynaptic proteins in lipid rafts during cortical development. Western blotting demonstrated that presynaptic proteins increased during the development of the cerebral cortex (data not shown). These results together suggest that lipid rafts and cholesterol biosynthesis play a crucial role in BDNF-induced synapse development.

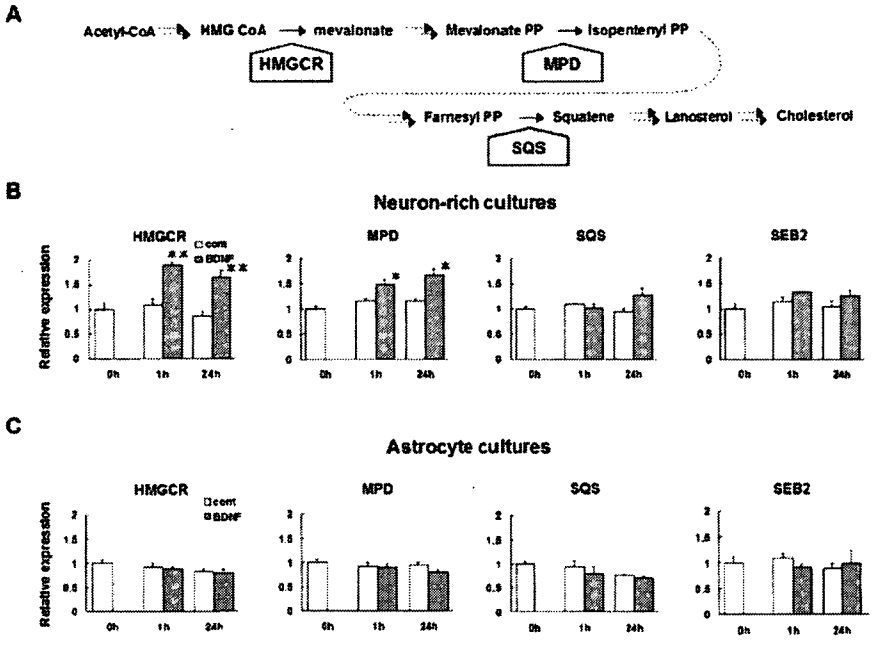

Figure 4. BDNF upregulates the mRNA levels of several cholesterol biosynthesis enzymes in neurons, but not in glial cells. ***A***, The mevalonate pathway in mammalian cells. Acetyl-CoA is converted to cholesterol via a pathway containing >20 enzymes (Goldstein et al., 2006). The enzymes in which the mRNA was measured are shown in bold. ***B***, ***C***, Cortical cells were cultured for 3 d in serum-containing medium. Astrocytes were cultured as described in Figure 3. The medium was changed to serum-free Neurobasal medium without the B27 supplement, and the cells were incubated overnight. On the next day, the cells were treated with 200 ng/ml BDNF for 0, 1, or 24 h, and total RNA was isolated. mRNAs of the indicated enzymes were quantified and normalized to that of GAPDH. Results shown are the means ± SEM from three or four mRNA preparations from independent culture dishes. Asterisks indicate a statistically significant difference from control cultures (Student's *t* test; $*p < 0.03$; $**p < 0.01$).

BDNF-elicited cholesterol biosynthesis increases neurotransmitter release by furnishing a readily releasable pool of synaptic vesicles

To elucidate further the physiological role of BDNF-elicited cholesterol biosynthesis on synaptic function, we performed whole-cell recordings on cultured hippocampal neurons (6–7 DIV), which increased cholesterol in response to BDNF (Fig. 1*B*). We first recorded spontaneous mEPSCs in the presence or absence of BDNF and/or mevastatin (Nakayama et al., 2005). The cultured hippocampal neurons at this stage, however, exhibited a very small number of mEPSCs (supplemental Fig. 1*A*, available at www.jneurosci.org as supplemental material). We found no significant effect of BDNF (200 ng/ml; 3 d) and/or mevastatin on the spontaneous synaptic transmission (supplemental Fig. 1*B*, available at www.jneurosci.org as supplemental material).

However, our previous results (Fig. 6) suggest that BDNF allows for the development of a presynaptic mechanism. It also was reported that endogenous BDNF promotes mobilization and/or docking of synaptic vesicles to presynaptic zones *in vivo* (Pozzo-Miller et al., 1999). We therefore speculated that BDNF may promote the development of a readily releasable pool (RRP) of synaptic vesicles, corresponding to docked synaptic vesicles (Rosenmund and Stevens, 1996). The docked vesicles are quantitated by the analysis of the neurotransmitter release evoked by hypertonic solutions containing sucrose, which elicits the fusion of a RRP of vesicles to the plasma membrane independently of intercellular Ca^{2+} concentration (Rosenmund and Stevens, 1996).

We cultured 3–4 DIV hippocampal neurons in the presence or absence of 200 ng/ml BDNF for 3 d, and at 6–7 DIV a hypertonic solution containing 100 mM sucrose was applied according to the method of Rosenmund and Stevens (1996). Remarkably, BDNF-treated neurons exhibited a robust increase in the event number of sucrose-evoked EPSCs under these conditions, whereas untreated cells showed no such response (Fig. 7*A*), suggesting that BDNF promotes the development of a RRP of vesicles, but not spontaneous neurotransmitter release, in cultured hippocampal neurons at this stage. Quantitative analysis demonstrated that the BDNF effect was significant (Fig. 7*B*,*C*) (BDNF at $p < 0.05$ compared with control).

We next examined the physiological role of BDNF-elicited cholesterol synthesis in the development of a RRP of vesicles. To this end we applied 10 μM mevastatin and 200 ng/ml BDNF for 3 d and analyzed the neurotransmitter release evoked by the hypertonic solution. Mevastatin prevented the BDNF-induced increase in the frequency of sucrose-evoked EPSCs (Fig. 7*B*,*C*) (BDNF plus mevastatin at $p < 0.05$ compared with BDNF at $p > 0.05$, compared with control). Treatment with mevastatin alone had no significant effect (Fig. 7*B*,*C*) (mevastatin at $p < 0.001$ compared with BDNF and at $p > 0.05$ compared with control). These data suggest that BDNF-elicited cholesterol biosynthesis is a crucial step in the maturation of RRP.

We also analyzed the amplitude of sucrose-evoked EPSCs (Fig. 7*B*,*D*). Pretreatment with BDNF increased the amplitude by 1.96 ± 0.27-fold (Fig. 7*D*) (BDNF at $p < 0.001$ as compared with control). However, mevastatin attenuated the amplitude increase by BDNF (Fig. 7*D*, BDNF plus mevastatin). Mevastatin alone had no significant effect (Fig. 7*D*). Hypertonic solution elicits a massive release of neurotransmitter from docked synaptic vesicles and leads to an increase in the amplitude of the EPSCs in a coincidental manner (Rosenmund and Stevens, 1996). These results suggest that BDNF promotes the development of presynaptic function involving a RRP of vesicles, rather than a postsynaptic function, by stimulating cholesterol biosynthesis.

Discussion

Accumulating evidence has demonstrated the association of defects in cholesterol homeostasis with neurological diseases (Maxfield and Tabas, 2005). In Huntington's disease (HD) the expanded glutamate tract in the huntingtin protein elicits neuronal cell death via the reduction of cholesterol biosynthesis (Valenza et al., 2005). The reduction of BDNF content in HD brains suggests a causal relationship between BDNF signaling and cholesterol metabolism (Zuccato et al., 2001).

Despite such evidence, the regulation of cholesterol metabolism in CNS neurons remains ill defined. The present study investigated the effect of BDNF on cholesterol biosynthesis in cultured CNS neurons. The results suggest that BDNF elicits cholesterol biosynthesis for the development of presynaptic functions.

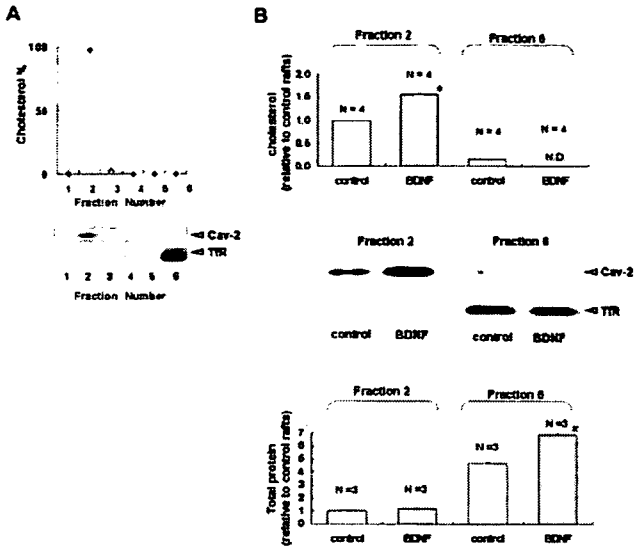

Figure 5. BDNF increases the amount of cholesterol and caveolin-2 in neuronal lipid rafts. Cortical neurons were cultured in the presence or absence of BDNF (200 ng/ml) for 3 d. ***A***, Lipid raft preparation. Cultured cortical neurons were homogenized in ice-cold lysis buffer containing Triton X-100 and centrifuged in discontinuous 5–35% sucrose gradients. Six fractions (from top to bottom) were collected. Top, The graph shows the cholesterol content in each fraction as a percentage of the total measured cholesterol, revealing peak cholesterol in the raft fraction (fraction 2). Bottom, Six fractions were separated on SDS-PAGE and immunoblotted for the indicated proteins. The lipid raft marker caveolin-2 is enriched in fraction 2, for which cholesterol concentration is the highest, whereas a nonraft marker protein, TfR, is concentrated in fraction 6. ***B***, Effect of BDNF on the amount of cholesterol, total protein, caveolin-2, and TfR. Fractions 2 and 6 were used to represent lipid rafts and nonraft domains, respectively. Top, BDNF significantly increased cellular cholesterol in the raft fraction, but not in the nonraft fraction. Results are presented relative to the control group in fraction 2. Middle, BDNF increased the amount of caveolin-2 in rafts but did not affect the distribution of the TfR. Bottom, BDNF significantly increased the total protein content of the nonraft fraction. Results are presented relative to the control group in fraction 2. The asterisks indicate a statistically significant difference from the control (Student's *t* test; $^*p < 0.001$).

BDNF regulates cholesterol biosynthesis in neurons

A key finding of this study is that long-term treatment with BDNF promotes cholesterol biosynthesis in neurons. To our knowledge, this is the first demonstration that growth factor regulates cholesterol biosynthesis in the CNS. This notion is confirmed by a number of biochemical studies: (1) two distinct quantitative methods revealed that BDNF led to a 15–40% increase in cholesterol content of cultured neurons; (2) BDNF upregulated the level of mRNA for cholesterol biosynthesis enzymes; (3) BDNF enhanced cholesterol biosynthesis in neurons, but not in glial cells; (4) pharmacological studies that used inhibitors of the cholesterol synthesis pathway additionally support the implications of this study; and (5) the notion that BDNF regulates cholesterol synthesis per se rather than mediating the redistribution of cholesterol inside cells was supported by the finding that BDNF-mediated increase in cholesterol biosynthesis still could be seen after normalizing for protein content, although whether the cholesterol synthesized in response to BDNF is redistributed from one region to another is an interesting but nonetheless ill-defined issue (Goldstein et al., 2006).

As shown previously (Reichardt, 2006), BDNF-induced TrkB activation is rapid and transient (supplemental Fig. 2, available at www.jneurosci.org as supplemental material). However, the effect of BDNF on cholesterol synthesis was significant after 3 d of treatment, suggesting that BDNF-dependent cholesterol synthesis can be categorized as a long-term effect of neurotrophins (Bibel and Barde, 2000). How the transient activation of the Trk receptor leads to a long-term effect of neurotrophins has been resolved only partially (Chao, 2003). There is substantial evidence demonstrating that (1) the morphological differentiation of pheochromocytoma (PC12) cells is accompanied by sustained Erk activity (Qui and Green, 1992) and that (2) ankyrin-rich membrane-spanning proteins play a role as scaffold molecules in the Trk receptor-dependent promotion of Erk activity (Arévalo et al., 2004). We reported that lipid rafts might be crucial for BDNF-dependent synaptic modulation, but not for neuronal survival (Suzuki et al., 2004). Future experiments will be designed to understand the signaling mechanism of BDNF-induced cholesterol biosynthesis.

Recently, the role of cholesterol in synapse development and synaptic function has been discussed extensively (Barres and Smith, 2001; Pfrieger, 2003). Mauch et al. (2001) demonstrated that glia-derived cholesterol enhances synaptogenesis, suggesting that the interaction between neurons and glial cells plays a crucial role in cholesterol-mediated synaptogenesis (Pfrieger, 2003). On the other hand, neurons themselves produce cholesterol and related molecules (Saito et al., 1987; Vance et al., 1994). Pharmacological inhibition of cholesterol biosynthesis affects axonal and dendritic morphogenesis (de Chaves et al., 1997; Fan et al., 2002; Pooler et al., 2006), and depletion of cholesterol by methyl-β-cyclodextrin reduces the number of hippocampal spines (Hering et al., 2003). The absence of the gene for cholesterol 24-hydroxylase causes significant defects in learning and memory (Kotti et al., 2006). The present study indicates that BDNF promotes synapse development via the stimulation of cholesterol biosynthesis and hypothesizes a novel role of neurotrophins on lipid metabolism in brain.

K252a, a general inhibitor of TrkB kinase activity, inhibited BDNF-induced cholesterol biosynthesis, suggesting that the BDNF/TrkB signaling is involved in cholesterol biosynthesis. In human fibroblasts platelet-derived growth factor (PDGF) treatment induces cholesterol biosynthesis via activation of phosphatidylinositol 3-kinase (Demoulin et al., 2004). However, treatment of cortical neuron cultures with a phosphatidylinositol 3-kinase inhibitor failed to suppress BDNF-induced cholesterol biosynthesis (BDNF and LY294002-treated/LY294002-treated; 1.22 ± 0.02; $p < 0.0001$), suggesting that the signaling pathway used by BDNF to activate cholesterol biosynthesis is different from that used by PDGF.

Twenty enzymes involved in cholesterol biosynthesis have been identified previously (Goldstein et al., 2006), suggesting the presence of a complex regulatory network controlling *de novo* cholesterol synthesis. We found that BDNF increased the transcription of genes encoding these enzymes in neurons, but not in glial cells. The significant and sustained increase in the level of the gene encoding HMGCR, the most rate-limiting enzyme of cholesterol synthesis (Goldstein et al., 2006), could lead to overall activation of cholesterol synthesis. Additionally, the genes studied here exhibited distinct time courses in their activations after BDNF stimulation (Fig. 4), suggesting that BDNF induces spatial and temporal regulation of the production of the intermediates of cholesterol synthesis (Goldstein et al., 2006).

Cholesterol synthesized in response to BDNF accumulates in lipid rafts: implications for synapse development

To understand the biological role of BDNF-promoted cholesterol biosynthesis, we tested whether BDNF promotes the accumulation of the newly synthesized cholesterol in rafts. Remarkably, BDNF increased the amount of cholesterol in the raft

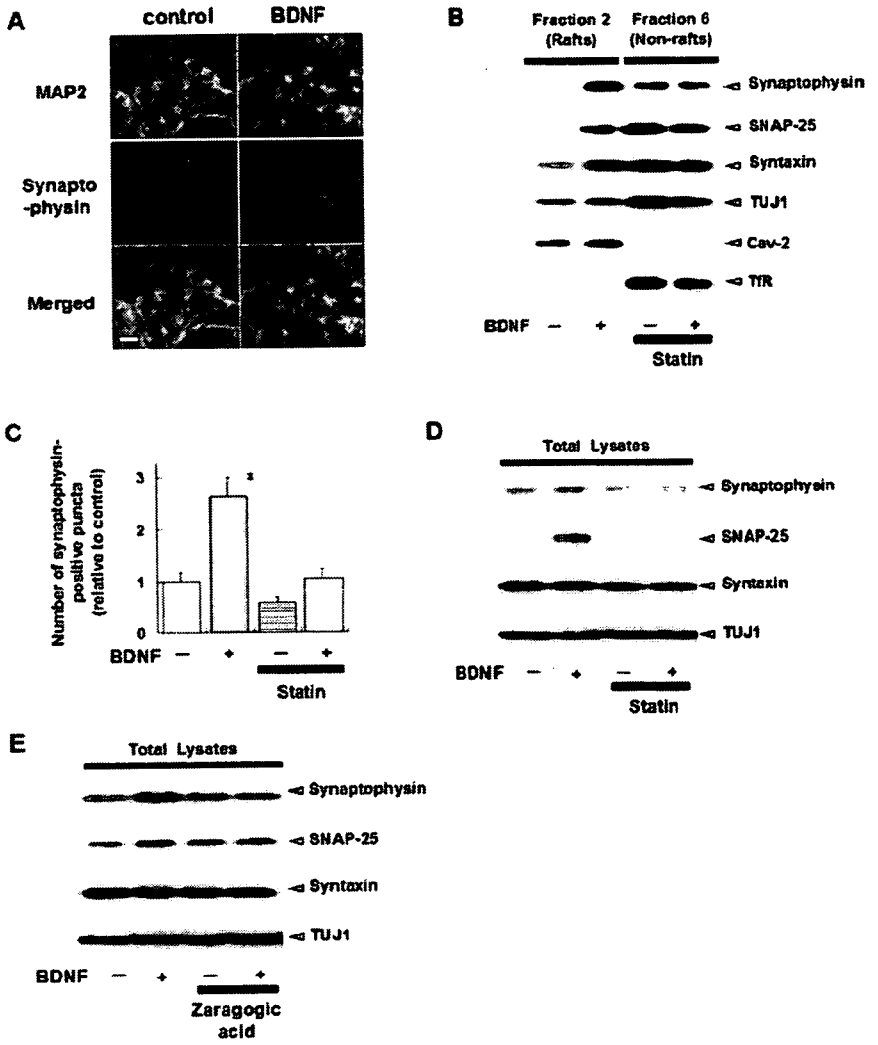

Figure 6. BDNF causes an increase in presynaptic proteins that accumulate in lipid rafts. Cortical neurons were cultured in the presence or absence of BDNF (200 ng/ml) and in the presence or absence of 10 μM mevastatin or 100 μM zaragozic acid for 3 d. ***A***, BDNF-increased the number of synaptophysin-positive puncta. Cortical neurons were stained by using antibodies against MAP-2 (green; neuron marker) and synaptophysin (red; presynaptic marker). Scale bar, 50 μm. ***B***, BDNF increases the presynaptic protein content of lipid rafts. Lipid raft and nonraft fractions were prepared as in Figure 5. Presynaptic proteins were detected with the indicated antibodies. ***C***, Effect of mevastatin on the BDNF-induced increase in presynaptic puncta. Immunostaining was performed as in ***A***. The synaptophysin-positive puncta were determined by using Scion Image as described in Materials and Methods. Results (the means ± SEM) are presented relative to −BDNF samples. The asterisk indicates a statistically significant difference from −BDNF samples (Student's *t* test; $*p < 0.01$). ***D***, ***E***, Cholesterol synthesis inhibitors prevent the BDNF-dependent increase in lipid raft-associated presynaptic proteins. Total cell lysates were immunoblotted with the indicated antibodies. The BDNF-dependent increase in presynaptic proteins was inhibited by mevastatin (***D***) and zaragozic acid (***E***).

fraction, but not in the nonraft fraction. Moreover, BDNF increased the level of the lipid raft-organizing protein caveolin-2 in rafts.

More intriguingly, BDNF restricted an increase in presynaptic proteins in lipid rafts, suggesting that cholesterol-rich lipid rafts play a crucial role on BDNF-induced synapse development. It was demonstrated that (1) cholesterol itself regulates the availability of synaptic vesicles via a direct interaction with synaptophysin (Thiele et al., 2000), (2) SNAP receptor (SNARE) complex formation is cholesterol-dependent (Lang et al., 2001; Mitter et al., 2003), and (3) the association of SNARE complex with lipid rafts regulates exocytosis (Salaſn et al., 2005). Presynaptic proteins are increased in cholesterol-rich lipid raft fractions concomitantly with cortical development (data not shown). Thus lipid rafts could provide an important structure for neurotransmitter release by promoting the interaction of cholesterol with synaptophysin or SNARE proteins.

Mevastain suppressed BDNF-induced increase in presynaptic proteins (Fig. 6*D*). Given that the mevalonate synthesis pathway through HMG-CoA regulates not only cholesterol synthesis but also isoprenoid production (Goldstein et al., 2006), mevastatin can suppress isoprenoid synthesis for the post-translational prenylation of cellular proteins such as Ras and Rho. However, the inhibitory effect of zaragozic acid on the BDNF-mediated increase in presynaptic proteins was comparable, but not partial, to that of mevastatin (Fig. 6*D*,*E*), leading to the interpretation that cholesterol synthesis, rather than isoprenoid synthesis, is crucial for synapse development.

BDNF elicits cholesterol synthesis for the development of a RRP of vesicles at presynaptic sites

Electrophysiological studies helped us to understand the role of BDNF-dependent cholesterol synthesis on synaptic development. First, although BDNF raised the number of synaptophysin-positive puncta and presynaptic proteins in hippocampal neurons (6–7 DIV), this effect was insufficient to provoke spontaneous mEPSCs. Remarkably, however, the electrophysiological study using hypertonic solution demonstrated that BDNF elicited exocytosis via a RRP of synaptic vesicles. This finding is conceptually consistent with a previous *in vivo* study that endogenous BDNF promotes the mobilization and/or docking of synaptic vesicles at presynaptic zones (Pozzo-Miller et al., 1999). Second, pretreatment with mevastatin prevented BDNF-dependent neurotransmitter release by a RRP of synaptic vesicles. Mevastatin itself did not affect sucrose-evoked EPSCs (Fig. 7*C*,*D*). These results together suggest that BDNF promotes the development of release machinery by the stimulation of cholesterol biosynthesis.

The full-length TrkB receptor is distributed at presynaptic and postsynaptic sites (Drake et al., 1999). It would be interesting to examine whether BDNF-promoted cholesterol biosynthesis stimulates the development of presynaptic and/or postsynaptic functions. Analysis of the neurotransmitter release evoked by a hypertonic solution (Rosenmund and Stevens, 1996) demonstrated that BDNF elicits a presynaptic function involving the exocytosis of a RRP of synaptic vesicles in developing neurons. On the other hand, BDNF had no significant effect on the amplitude of spontaneous mEPSCs (supplemental Fig. 1*B*, right, available at www.jneurosci.org as supplemental material), suggesting that BDNF is insufficient for the development of postsynaptic function at the developing stage. Additionally, a pharmacological

study using mevastatin indicated that neither cholesterol nor BDNF-induced cholesterol synthesis had any effect on the amplitude of mEPSPs at postsynaptic sites (supplemental Fig. 1*B*, right, available at www.jneurosci.org as supplemental material). In marked contrast, mature hippocampal neurons regulate the shape and number of dendritic spines via cholesterol synthesis (Hering et al., 2003). To our knowledge the finding that BDNF-promoted cholesterol synthesis mediates a presynaptic function involving the exocytosis of a RRP of vesicles in developing neurons constitutes a novel mechanism for synapse development.

Recent reviews have highlighted a role for cholesterol-rich lipid rafts in neurotrophin signaling (Paratcha and Ibanez, 2002; Nagappan and Lu, 2005). In the present study, we demonstrated that BDNF acts as a novel regulator of cholesterol biosynthesis. BDNF also promoted the accumulation of presynaptic proteins in cholesterol-rich lipid rafts. Cholesterol and BDNF-dependent cholesterol biosynthesis may play an important role in presynaptic development. It will be important to determine how cholesterol-rich lipid rafts furnish a functional platform for presynaptic sites. Gaining a more profound understanding of the mechanisms by which neurotrophins regulate lipid metabolism is an important and intriguing issue that will provide a framework for future studies.

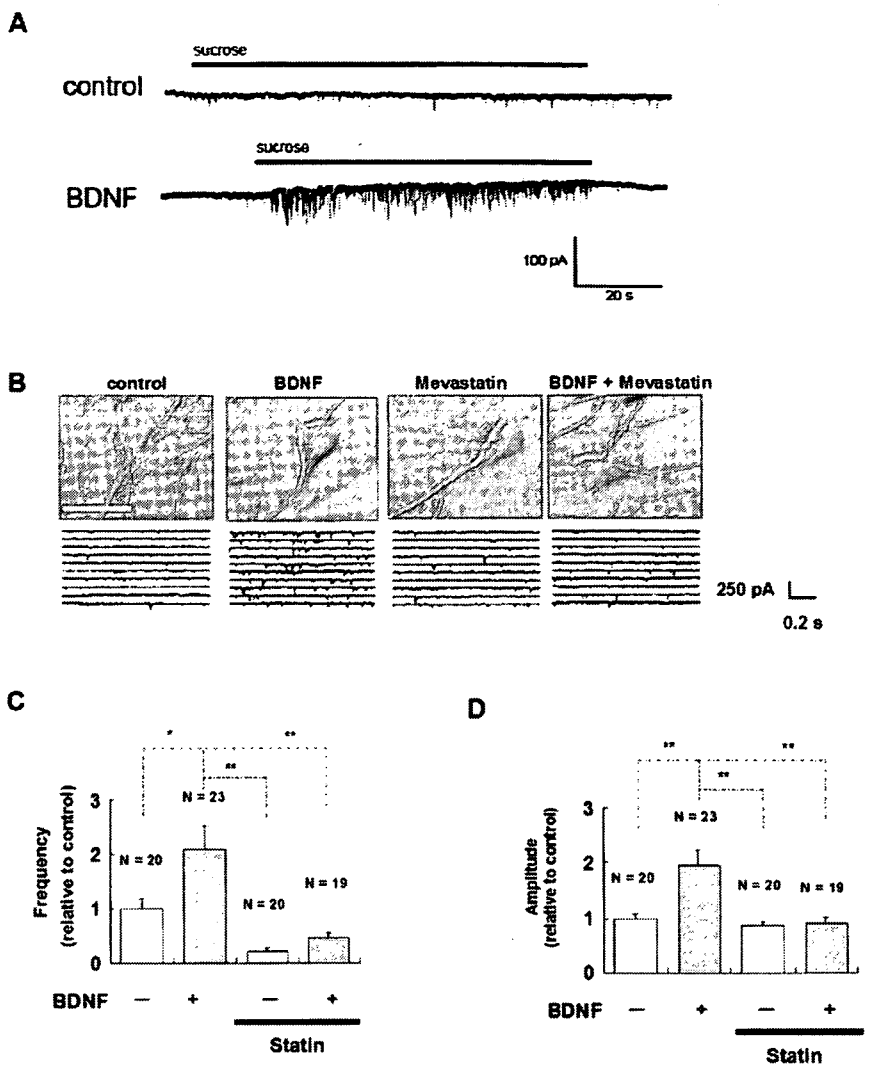

Figure 7. Effect of BDNF and/or mevastatin on a RRP of synaptic vesicles. Cultured hippocampal neurons (3–4 DIV) were treated with or without BDNF (200 ng/ml) and/or 10 μM mevastatin for 3 d. At 6–7 DIV, the hypertonic solution containing 100 mM sucrose was applied for recording sucrose-evoked EPSCs. This solution was applied to neurons for 35 s, and the recording was started 5 s after each stimulation in ***A–D***. ***A***, Representative traces of sucrose-evoked EPSCs in control and BDNF-treated neurons. Horizontal bar indicates the duration of perfusion of 100 mM sucrose. Note that there is a striking difference in the trace of sucrose-evoked responses between the BDNF-treated cell and the control cell. ***B***, Sucrose-evoked responses from neurons treated with the indicated drugs. Top, Representative images of the neurons treated with the indicated drugs. Scale bar, 30 μm. Bottom, Representative traces of sucrose-evoked EPSCs in cultured hippocampal neurons treated with the indicated drugs. ***C***, ***D***, Summary of the frequency and amplitude of sucrose-evoked EPSCs. Data were normalized to that of control neurons (−BDNF; −Statin); *n* = the number of independent coverslips. Asterisks indicate a statistically significant difference from control neurons (one-way ANOVA, followed by *post hoc* test; $*p < 0.05$; $**p < 0.001$).

References

Arévalo JC, Yano H, Teng KK, Chao MV (2004) A unique pathway for sustained neurotrophin signaling through an ankyrin-rich membrane-spanning protein. EMBO J 23:2358–2368.

Barres BA, Smith SJ (2001) Neurobiology. Cholesterol—making or breaking the synapse. Science 294:1296–1297.

Bergstrom JD, Kurtz MM, Rew DJ, Amend AM, Karkas JD, Bostedor RG, Bansal VS, Dufresne C, VanMiddlesworth FL, Hensens OD, Liesch JM, Zink DL, Wilson KE, Onishi J, Milligan JA, Bills G, Kaplan L, Omstead MN, Jenkins RG, Huang L, et al. (1993) Zaragozic acids: a family of fungal metabolites that are picomolar competitive inhibitors of squalene synthase. Proc Natl Acad Sci USA 90:80–84.

Bibel M, Barde YA (2000) Neurotrophins: key regulators of cell fate and cell shape in the vertebrate nervous system. Genes Dev 14:2919–2937.

Brewer GJ, Torricelli JR, Evege EK, Price PJ (1993) Optimized survival of hippocampal neurons in B27-supplemented Neurobasal, a new serum-free medium combination. J Neurosci Res 35:567–576.

Brown MS, Goldstein JL (1999) A proteolytic pathway that controls the cholesterol content of membranes, cells, and blood. Proc Natl Acad Sci USA 96:11041–11048.

Chao MV (2003) Neurotrophins and their receptors: a convergence point for many signaling pathways. Nat Rev Neurosci 4:299–309.

de Chaves EI, Rusinol AE, Vance DE, Campenot RB, Vance JE (1997) Role of lipoproteins in the delivery of lipids to axons during axonal regeneration. J Biol Chem 272:30766–30773.

Demoulin JB, Ericsson J, Kallin A, Rorsman C, Ronnstrand L, Heldin CH (2004) Platelet-derived growth factor stimulates membrane lipid synthesis through activation of phosphatidylinositol 3-kinase and sterol regulatory element-binding proteins. J Biol Chem 279:35392–35402.

Drake CT, Milner TA, Patterson SL (1999) Ultrastructural localization of full-length TrkB immunoreactivity in rat hippocampus suggests multiple roles in modulating activity-dependent synaptic plasticity. J Neurosci 19:8009–8026.

Fan QW, Yu W, Gong JS, Zou K, Sawamura N, Senda T, Yanagisawa K, Michikawa M (2002) Cholesterol-dependent modulation of dendrite outgrowth and microtubule stability in cultured neurons. J Neurochem 80:178–190.

Figurov A, Pozzo-Miller LD, Olafsson P, Wang T, Lu B (1996) Regulation of synaptic responses to high-frequency stimulation and LTP by neurotrophins in the hippocampus. Nature 381:706–709.

Goldstein JL, DeBose-Boyd RA, Brown MS (2006) Protein sensors for membrane sterols. Cell 124:35–46.

Guirland C, Suzuki S, Kojima M, Lu B, Zheng JQ (2004) Lipid rafts mediate chemotropic guidance of nerve growth cones. Neuron 42:51–62.

Hering H, Lin CC, Sheng M (2003) Lipid rafts in the maintenance of synapses, dendritic spines, and surface AMPA receptor stability. J Neurosci 23:3262–3271.

Kotti TJ, Ramirez DM, Pfeiffer BE, Huber KM, Russell DW (2006) Brain cholesterol turnover required for geranylgeraniol production and learning in mice. Proc Natl Acad Sci USA 103:3869–3874.

Krijnse-Locker J, Parton RG, Fuller SD, Griffiths G, Dotti CG (1995) The organization of the endoplasmic reticulum and the intermediate compartment in cultured rat hippocampal neurons. Mol Biol Cell 6:1315–1332.

Lang T, Bruns D, Wenzel D, Riedel D, Holroyd P, Thiele C, Jahn R (2001) SNAREs are concentrated in cholesterol-dependent clusters that define docking and fusion sites for exocytosis. EMBO J 20:2202–2213.

Lessmann V (1998) Neurotrophin-dependent modulation of glutamatergic synaptic transmission in the mammalian CNS. Gen Pharmacol 31:667–674.

Ma L, Huang YZ, Pitcher GM, Valtschanoff JG, Ma YH, Feng LY, Lu B, Xiong WC, Salter MW, Weinberg RJ, Mei L (2003) Ligand-dependent recruitment of the ErbB4 signaling complex into neuronal lipid rafts. J Neurosci 23:3164–3175.

Mauch DH, Nagler K, Schumacher S, Goritz C, Muller EC, Otto A, Pfrieger FW (2001) CNS synaptogenesis promoted by glia-derived cholesterol. Science 294:1354–1357.

Maxfield FR, Tabas I (2005) Role of cholesterol and lipid organization in disease. Nature 438:612–621.

McAllister AK, Lo DC, Katz LC (1995) Neurotrophins regulate dendritic growth in developing visual cortex. Neuron 15:791–803.

Metherall JE, Waugh K, Li H (1996) Progesterone inhibits cholesterol biosynthesis in cultured cells. Accumulation of cholesterol precursors. J Biol Chem 271:2627–2633.

Mitter D, Reisinger C, Hinz B, Hollmann S, Yelamanchili SV, Treiber-Held S, Ohm TG, Herrmann A, Ahnert-Hilger G (2003) The synaptophysin/synaptobrevin interaction critically depends on the cholesterol content. J Neurochem 84:35–42.

Nagappan G, Lu B (2005) Activity-dependent modulation of the BDNF receptor TrkB: mechanisms and implications. Trends Neurosci 28:464–471.

Nakayama K, Kiyosue K, Taguchi T (2005) Diminished neuronal activity increases neuron–neuron connectivity underlying silent synapse formation and the rapid conversion of silent to functional synapses. J Neurosci 25:4040–4051.

Ohira K, Kumanogoh H, Sahara Y, Homma KJ, Hirai H, Nakamura S, Hayashi M (2005) A truncated tropomyosin-related kinase B receptor, T1, regulates glial cell morphology via Rho GDP dissociation inhibitor 1. J Neurosci 25:1343–1353.

Paratcha G, Ibanez CF (2002) Lipid rafts and the control of neurotrophic factor signaling in the nervous system: variations on a theme. Curr Opin Neurobiol 12:542–549.

Patterson SL, Abel T, Deuel TA, Martin KC, Rose JC, Kandel ER (1996) Recombinant BDNF rescues deficits in basal synaptic transmission and hippocampal LTP in BDNF knockout mice. Neuron 16:1137–1145.

Pereira DB, Chao MV (2007) The tyrosine kinase Fyn determines the localization of TrkB receptors in lipid rafts. J Neurosci 27:4859–4869.

Pfrieger FW (2003) Role of cholesterol in synapse formation and function. Biochim Biophys Acta 1610:271–280.

Poo MM (2001) Neurotrophins as synaptic modulators. Nat Rev Neurosci 2:24–32.

Pooler AM, Xi SC, Wurtman RJ (2006) The 3-hydroxy-3-methylglutaryl coenzyme A reductase inhibitor pravastatin enhances neurite outgrowth in hippocampal neurons. J Neurochem 97:716–723.

Pozzo-Miller LD, Gottschalk W, Zhang L, McDermott K, Du J, Gopalakrishnan R, Oho C, Sheng ZH, Lu B (1999) Impairments in high-frequency transmission, synaptic vesicle docking, and synaptic protein distribution in the hippocampus of BDNF knockout mice. J Neurosci 19:4972–4983.

Qui MS, Green SH (1992) PC12 cell neuronal differentiation is associated with prolonged $p21^{ras}$ activity and consequent prolonged ERK activity. Neuron 9:705–717.

Rasika S, Alvarez-Buylla A, Nottebohm F (1999) BDNF mediates the effects of testosterone on the survival of new neurons in an adult brain. Neuron 22:53–62.

Reichardt LF (2006) Neurotrophin-regulated signaling pathways. Philos Trans R Soc Lond B Biol Sci 361:1545–1564.

Rose CR, Blum R, Pichler B, Lepier A, Kafitz KW, Konnerth A (2003) Truncated TrkB-T1 mediates neurotrophin-evoked calcium signaling in glia cells. Nature 426:74–78.

Rosenmund C, Stevens CF (1996) Definition of the readily releasable pool of vesicles at hippocampal synapses. Neuron 16:1197–1207.

Saito M, Benson EP, Saito M, Rosenberg A (1987) Metabolism of cholesterol and triacylglycerol in cultured chick neuronal cells, glial cells, and fibroblasts: accumulation of esterified cholesterol in serum-free culture. J Neurosci Res 18:319–325.

Salaſn C, Gould GW, Chamberlain LH (2005) Lipid raft association of SNARE proteins regulates exocytosis in PC12 cells. J Biol Chem 280:19449–19453.

Shimano H (2001) Sterol regulatory element-binding proteins (SREBPs): transcriptional regulators of lipid synthetic genes. Prog Lipid Res 40:439–452.

Simons K, Toomre D (2000) Lipid rafts and signal transduction. Nat Rev Mol Cell Biol 1:31–39.

Suzuki S, Mizutani M, Suzuki K, Yamada M, Kojima M, Hatanaka H, Koizumi S (2002) Brain-derived neurotrophic factor promotes interaction of the Nck2 adaptor protein with the TrkB tyrosine kinase receptor. Biochem Biophys Res Commun 294:1087–1092.

Suzuki S, Numakawa T, Shimazu K, Koshimizu H, Hara T, Hatanaka H, Mei L, Lu B, Kojima M (2004) BDNF-induced recruitment of TrkB receptor into neuronal lipid rafts: roles in synaptic modulation. J Cell Biol 167:1205–1215.

Tacer KF, Haugen TB, Baltsen M, Debeljak N, Rozman D (2002) Tissue-specific transcriptional regulation of the cholesterol biosynthetic pathway leads to accumulation of testis meiosis-activating sterol (T-MAS). J Lipid Res 43:82–89.

Takamori S, Holt M, Stenius K, Lemke EA, Gronborg M, Riedel D, Urlaub H, Schenck S, Brugger B, Ringler P, Muller SA, Rammner B, Grater F, Hub JS, De Groot BL, Mieskes G, Moriyama Y, Klingauf J, Grubmuller H, Heuser J, et al. (2006) Molecular anatomy of a trafficking organelle. Cell 127:831–846.

Takei N, Sasaoka K, Inoue K, Takahashi M, Endo Y, Hatanaka H (1997) Brain-derived neurotrophic factor increases the stimulation-evoked release of glutamate and the levels of exocytosis-associated proteins in cultured cortical neurons from embryonic rats. J Neurochem 68:370–375.

Takei N, Kawamura M, Hara K, Yonezawa K, Nawa H (2001) Brain-derived neurotrophic factor enhances neuronal translation by activating multiple initiation processes: comparison with the effects of insulin. J Biol Chem 276:42818–42825.

Tapley P, Lamballe F, Barbacid M (1992) K252a is a selective inhibitor of the tyrosine protein kinase activity of the Trk family of oncogenes and neurotrophin receptors. Oncogene 7:371–381.

Tartaglia N, Du J, Tyler WJ, Neale E, Pozzo-Miller L, Lu B (2001) Protein synthesis-dependent and -independent regulation of hippocampal synapses by brain-derived neurotrophic factor. J Biol Chem 276:37585–37593.

Thiele C, Hannah MJ, Fahrenholz F, Huttner WB (2000) Cholesterol binds to synaptophysin and is required for biogenesis of synaptic vesicles. Nat Cell Biol 2:42–49.

Valenza M, Rigamonti D, Goffredo D, Zuccato C, Fenu S, Jamot L, Strand A, Tarditi A, Woodman B, Racchi M, Mariotti C, Di Donato S, Corsini A, Bates G, Pruss R, Olson JM, Sipione S, Tartari M, Cattaneo E (2005) Dysfunction of the cholesterol biosynthetic pathway in Huntington's disease. J Neurosci 25:9932–9939.

Vance JE, Pan D, Campenot RB, Bussiere M, Vance DE (1994) Evidence that the major membrane lipids, except cholesterol, are made in axons of cultured rat sympathetic neurons. J Neurochem 62:329–337.

Vance JE, Hayashi H, Karten B (2005) Cholesterol homeostasis in neurons and glial cells. Semin Cell Dev Biol 16:193–212.

Wang T, Xie K, Lu B (1995) Neurotrophins promote maturation of developing neuromuscular synapses. J Neurosci 15:4796–4805.

Zuccato C, Ciammola A, Rigamonti D, Leavitt BR, Goffredo D, Conti L, MacDonald ME, Friedlander RM, Silani V, Hayden MR, Timmusk T, Sipione S, Cattaneo E (2001) Loss of huntingtin-mediated BDNF gene transcription in Huntington's disease. Science 293:493–498.

Cell PRESS

Regulation of Dendritogenesis via a Lipid-Raft-Associated Ca^{2+}/Calmodulin-Dependent Protein Kinase CLICK-III/CaMKIγ

Sayaka Takemoto-Kimura,[1,7] Natsumi Ageta-Ishihara,[1,2,7] Mio Nonaka,[1] Aki Adachi-Morishima,[1] Tatsuo Mano,[1] Michiko Okamura,[1] Hajime Fujii,[1] Toshimitsu Fuse,[1,2] Mikio Hoshino,[3] Shingo Suzuki,[4,6] Masami Kojima,[4,6] Masayoshi Mishina,[5,6] Hiroyuki Okuno,[1] and Haruhiko Bito[1,2,6,*]

[1] Department of Neurochemistry

[2] The Center for Integrated Brain Medical Science

Graduate School of Medicine, The University of Tokyo, Bunkyo-ku, Tokyo 113-0033, Japan

[3] Department of Pathology and Tumor Biology, Graduate School of Medicine, Kyoto University, Sakyo-ku, Kyoto 606-8501, Japan

[4] Research Institute for Cell Engineering, National Institute of Advanced Industrial Science and Technology (AIST), Ikeda, Osaka, 563-8577, Japan

[5] Department of Molecular Neurobiology and Pharmacology, Graduate School of Medicine, the University of Tokyo, Bunkyo-ku, Tokyo 113-0033, Japan

[6] SORST-JST, Kawaguchi 332-0012, Japan

[7] These authors contributed equally to this work.

*Correspondence: hbito@m.u-tokyo.ac.jp

DOI 10.1016/j.neuron.2007.05.021

SUMMARY

Ca^{2+} signaling plays a central role in activity-dependent regulation of dendritic arborization, but key molecular mechanisms downstream of calcium elevation remain poorly understood. Here we show that the C-terminal region of the Ca^{2+}/calmodulin-dependent protein kinase CLICK-III (CL3)/CaMKIγ, a membrane-anchored CaMK, was uniquely modified by two sequential lipidification steps: prenylation followed by a kinase-activity-regulated palmitoylation. These modifications were essential for CL3 membrane anchoring and targeting into detergent-resistant lipid microdomains (or rafts) in the dendrites. We found that CL3 critically contributed to BDNF-stimulated dendritic growth. Raft insertion of CL3 specifically promoted dendritogenesis of cortical neurons by acting upstream of RacGEF STEF and Rac, both present in lipid rafts. Thus, CL3 may represent a key element in the Ca^{2+}-dependent and lipid-raft-delineated switch that turns on extrinsic activity-regulated dendrite formation in developing cortical neurons.

INTRODUCTION

Neurons grow two characteristic processes: axons and dendrites. The specification of these processes, their outgrowth, and their precise arborization are prerequisites for the formation of appropriate connections between neurons. These steps, which constitute the basis for the establishment of neuronal circuits, represent central questions in neuroscience for which the molecular mechanisms still remain largely unsolved.

The dendrite formation, which is critical for proper integration of synaptic inputs, is believed to be determined by genetically encoded cell-intrinsic signals as well as environmental-extrinsic signals from neighboring cells. Recent works have shed light on the critical roles of semaphorin 3A, neurotrophins, Notch1, Slit-1, cadherin, BMP, and Wnt/β-catenin in mediating signaling events regulating various stages of dendritogenesis in the developing cerebral cortex (reviewed in Ciani and Salinas, 2005; Higgins et al., 1997; Jan and Jan, 2003; Whitford et al., 2002). In addition, a wealth of work has shown that the formation of dendritic trees is shaped by neuronal activity (Cline, 2001; Konur and Ghosh, 2005). For example, surgical and pharmacological attenuation of sensory inputs impaired dendritic development in the visual cortex as well as in the barrel cortex (Fox and Wong, 2005), while in contrast, enriched environments promoted dendritic growth (Kozorovitskiy et al., 2005). However, how neural activity regulates dendrite arborization at the molecular and cellular level is not well understood.

Activity-dependent regulation of dendritic arbors is believed to be mediated, in large part, via increases in intracellular calcium concentration, which in turn activate several signaling cascades. How can neuronal activity influence dendrite formation downstream of calcium entry and mobilization? Several works have so far indicated a possible involvement of one or multiple members of the multifunctional Ca^{2+}/calmodulin (CaM)-dependent protein kinases (CaMKs) family in dendritic development. CaMKs represent major targets for an activated Ca^{2+}/CaM complex generated by intracellular calcium rise, and two subclasses (the CaMKI/IV subfamily [consisting

of five genes] and a CaMKII subfamily [consisting of four genes]) have been shown to be highly expressed in the central nervous system (CNS) (Soderling and Stull, 2001; Hook and Means, 2001; Hudmon and Schulman, 2002). The general CaMK inhibitor KN-62, which inhibited activation of members of both kinase subclasses, was shown to block neurite outgrowth in various cell lines (Zheng et al., 1994; Kuhn et al., 1998; Vaillant et al., 2002). The role of CaMKII in neurite outgrowth has been controversial, however, in part because of the contrasting effect observed between the α and β isoforms of CaMKII (Konur and Ghosh, 2005). CaMKIV, enriched in the nucleus, was shown to mediate dendrite formation via CREB phosphorylation and CREB-mediated transcription (Redmond et al., 2002). Additionally, CaMKI activity may participate in the regulation of growth cone motility and neurite extension (Wayman et al., 2004; Schmitt et al., 2004), but the underlying isoforms and critical mechanisms involved remained obscure.

Recently, a variety of Rho small GTPase family proteins were shown to contribute to dendritic morphogenesis through regulation of actin cytoskeletal remodeling (Luo, 2002; Van Aelst and Cline, 2004). How the small GTPase activity was turned on and off as a function of neuronal activity and multiple coexisting extracellular cues remained largely unknown. In some instances, the GDP-GTP exchange factor (GEF) for a Rho small GTPase family protein was shown to be activated downstream of Ca^{2+}. Thus, a synaptically localized Rac-GEF Tiam1 was involved in the regulation of dendritic spines by linking NMDA-receptor activity to Rac1-dependent actin remodeling (Tolias et al., 2005). However, it was not known whether nor which specific CaMK activity may contribute to small GTPase-dependent dendritic actin remodeling during dendritogenesis.

Here, we show a unique function of a lipid-raft-associated Ca^{2+}/calmodulin-dependent protein kinase, CLICK-III (CL3)/CaMKIγ, in dendritogenesis of developing cortical neurons. The C-terminal end of CL3 was the substrate for sequential lipidifications, i.e., prenylation and palmitoylation. Prenyl-palmitoyl-CL3, generated in a kinase-activity-dependent manner, efficiently accumulated into dendrite-enriched raft-like lipid microdomains. Intriguingly, knockdown or knockout of CL3 reduced the number and the total length of dendrites, but not those of axons. Furthermore, blockade of CL3 occluded BDNF-stimulated dendritic growth, and CL3 membrane anchoring appeared to play an important role in mediating this morphological effect. In keeping with the critical significance of raft insertion of CL3, Rac and its upstream regulator STEF, a Rac-specific GEF, acted downstream of CL3 in the molecular cascade linking Ca^{2+} to actin remodeling, and both were present in the lipid rafts. Consistent with these results, Rac activity was sufficient to rescue the dendritic phenotype associated with CL3 knockdown, while raft disruption abolished the dendritogenic effect of CL3 overexpression. Taken together, we thus uncovered a novel CaMK-Rac signaling pathway by which lipid raft insertion and activation of a specific CaMKI isoform may couple extrinsic neuronal activity with dendrite-restricted cytoskeletal remodeling in developing cortical neurons.

RESULTS

Prenylated CL3 Is Palmitoylated in a Kinase-Activity-Dependent Manner and This Dual Lipidification Determines Golgi Membrane Anchoring and Dendrite-Enriched Lipid Raft Targeting

Prenylation was often reported to be accompanied by palmitoylation in many neuronal proteins (El-Husseini and Bredt, 2002). We directly tested the presence of multiple palmitoylation sites in the vicinity of the CAAX motif of CL3/CaMKIγ, a membrane-anchored CaMK (Takemoto-Kimura et al., 2003) (Figure 1A). Tritiated precursors for either prenyl or palmitoyl moieties, [^{3}H]-mevalonate or [^{3}H]-palmitate, were added in the culture medium of COS-7 cells expressing either wild-type (WT) CL3 or various C-to-S substitution mutants of CL3, and lipidification of CL3 was tested using SDS-PAGE and digital autoradiography. Either [^{3}H]-mevalonate conjugation or [^{3}H]-palmitate incorporation was significantly detected in WT-expressing cells (Figures 1B and 1C, WT). The former was absent in a C474S mutant (Figure 1B, C474S), consistent with a CAAX prenylation. In contrast, the latter was reduced to background levels in a quadruple mutation (4CS) of four cysteines (C417S, C419S, C420S, and C423S) (Figure 1C, 4CS), identifying these residues as potential palmitoylation sites.

We next tested whether there was a possible interaction between prenylation, palmitoylation, and kinase activity. Interestingly, the 4CS mutant was prenylated to a similar extent as the WT CL3 (Figure 1D), while palmitoylation was hardly detected in a prenylation-deficient C474S mutant (Figure 1E). Thus, prenylation and palmitoylation might take place in a series, with prenylation perhaps occurring prior to and as a prerequisite for palmitoylation. Furthermore, a K52A kinase-inactive mutant of CL3, in which the consensus ATP-binding lysine residue was replaced with an alanine, was prenylated as much as the WT (Figure 1D), but its palmitoylation was significantly impaired (Figure 1E). These lines of evidence suggested that kinase activation on a prenylated (and thus presumably membrane inserted) CL3 may perhaps trigger a robust conformational change near the membranes that is necessary for full palmitoylation.

Recently, 23 palmitoyl acyl transferases (PATs) have been identified (Fukata et al., 2004; Linder and Deschenes, 2004). The brain-specific localization and the Golgi enrichment of a PAT, originally identified as a Golgi-apparatus-specific protein with the DHHC zinc finger domain (GODZ) (Uemura et al., 2002), were reminiscent of the distribution of CL3. We therefore tested whether GODZ might palmitoylate CL3. GODZ coexpression with CL3 in heterologous cells yielded a 4.3-fold

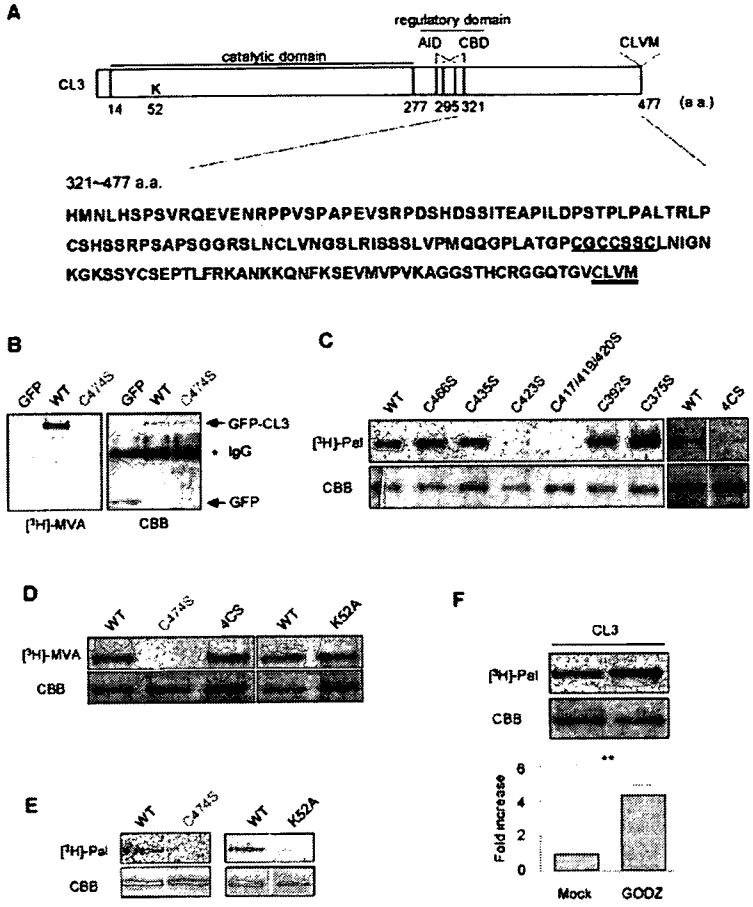

Figure 1. The C-Terminal Region of CL3 Is Covalently Modified by a Dual Lipidification Mechanism that Involves Prenylation of the CAAX Motif and a Subsequent Activity-Regulated Palmitoylation

(A) Domain structure of CL3 (upper panel) and amino acid sequence of its C-terminal end (lower panel). The numbers show the position of amino acid residues. In addition to a classical prenylation site at the Cys-474 residue (in blue) of the C-terminal CAAX motif (double underline), the unique C-terminal region of CL3 contained multiple Cys residues (in red and green), which constituted potential palmitoylation sites. Among them, four neighboring Cys (in red and underlined) were experimentally validated as critical residues for palmitoylation, as shown also in (C). AID, autoinhibitory domain; CBD, Ca^{2+}/calmodulin-binding domain.

(B) Prenylation of the CAAX motif of CL3. Immunoprecipitates for each sample were obtained using an anti-GFP antibody and examined by SDS-PAGE followed by autoradiographic exposure. [^{3}H]-mevalonate ([^{3}H]-MVA) incorporation (left) was detected in a wild-type GFP-CL3 (WT), but not in a CAAX motif mutant (C474S) or GFP alone. The amount of loaded proteins in each lane was comparable, as shown by CBB staining (right). The mobility of GFP-CL3 and GFP are indicated by arrows, and the heavy chain of the IgG used for immunoprecipitation is shown by an asterisk.

(C) Determination of critical palmitoylated Cys residues on CL3. Incorporation of [^{3}H]-palmitate ([^{3}H]-Pal) was observed in wild-type GFP-CL3 (WT). Incorporation of [^{3}H]-palmitate was significantly diminished in two mutants (in red), C417/419/420S (triple Cys-to-Ser substitution at residues 417, 419, and 420) and C423S, indicating the existence of multiple Cys residues critical for palmitoylation. Unaffected mutants are shown in green. A quadruple mutant (4CS) with a quadruple substitution had the least amount of [^{3}H]-palmitate incorporation and was considered to be a palmitoylation-deficient mutant (4CS).

(D) Unchanged level of prenylation on both a palmitoylation-deficient (4CS) and a kinase-dead (K52A, a Lys residue in the ATP-binding pocket replaced with an Ala) mutant of CL3.

(E) A decrease in palmitoylation was observed in a prenylation-deficient mutant (C474S), as well as a kinase-inactive mutant (K52A).

(F) Coexpression of HA-GODZ, a neuronal palmitoyl acyl transferase, led to a significant increase in CL3 palmitoylation by 4.32 ± 0.55 fold (n = 5). **$p < 0.01$ by paired t test.

increase (4.3 ± 0.55, n = 5) in the amount of palmitate incorporation (Figure 1F).

We previously found that prenylation per se may be necessary for membrane anchoring and for trafficking to diverse membrane compartments, such as the Golgi apparatus or the plasma membranes (Takemoto-Kimura et al., 2003). To test whether an additional palmitoylation may help to redistribute CL3 into specific membrane signalosomes such as those enriched at lipid rafts (Anderson and Jacobson, 2002), we expressed GFP-tagged CL3 (GFP-CL3) in cultured cortical neurons using a lentiviral vector driven by a synapsin I promoter. Consistent with our hypothesis, CL3 cofractionated with the lipid raft markers, caveolin-2 and flotillin-1, in the Triton X-100-insoluble low-density membrane fractions (Figure 2A). We next directly visualized raft-inserted CL3 localization in cultured neurons treated with 0.1% Triton X-100, as any residual GFP signal should then be indicative of the presence of CL3 in detergent-resistant membrane microdomains. In keeping with this, a sizable detergent nonextractable pool of GFP-CL3 was present in the perinuclear Golgi and proximal dendrites in developing hippocampal neurons (see Figure S1A in the Supplemental Data available with this article online, -GODZ arrow and arrowhead; and Figure S1B), and this pool was further increased by coexpression of GODZ (Figure S1A, +GODZ arrow and arrowheads). In immature cortical neurons, a large majority of the CL3 signal that was resistant to detergent treatment was present both in the intracellular perinuclear Golgi-like membranes and in the minor processes (i.e., dendrites) (Figure 2B, upper panel, see line scan in the inset for CL3 signal in the dendrites). Importantly, this detergent-resistant pool of CL3 was almost completely lost when neurons were treated with zaragozic acid, an

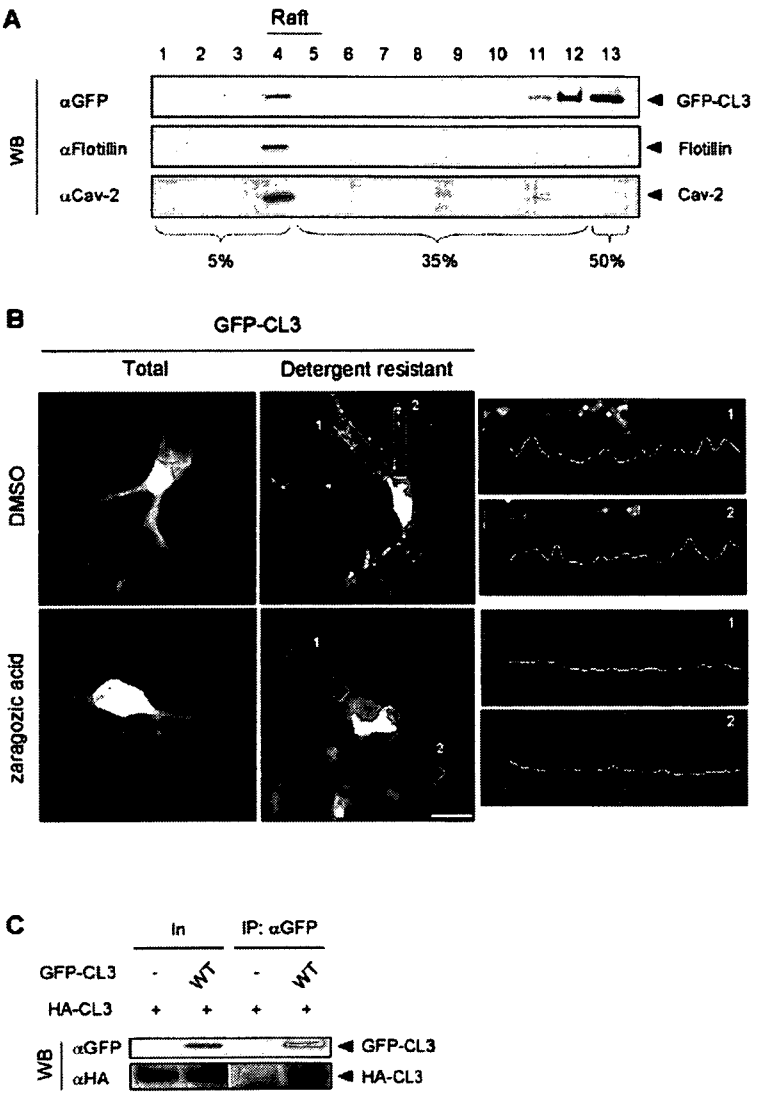

Figure 2. Dendritic Raft Targeting and Multimeric Complex Formation of CL3 in Cortical Neurons

(A) Wild-type GFP-CL3 (WT) expressed in cortical neurons using a synapsin I promoter-driven lentivirus was recovered in the lipid raft fraction (lanes 4–5), as confirmed by the enrichment of raft marker proteins flotillin-1 and caveolin-2 (Cav-2). Fractions 1–4, 5% sucrose; 5–12, 35% sucrose; 13, 50% sucrose.

(B) A sizable portion of total GFP-CL3 fluorescence was recovered after detergent treatment as detergent-resistant GFP-CL3, which was localized in a punctate manner in 2 DIV cortical neurons along the dendrites as well as at the perinuclear region. Dendrites were unambiguously identified as processes of limited length (much shorter than the axon exceeding 100 μm). Line scans of pixel fluorescence, carried out within a chosen field of a 15 μm dendritic segment (in insets 1 and 2) by horizontally tracking the clusters of GFP-CL3, illustrate the spotty presence of raft-inserted CL3 along the dendrites (right panels). Treatment with 100 μM zaragozic acid abolished the dendritic detergent-resistant patches and flattened the line scan profile. Scale bar, 10 μm.

(C) CL3 forms a multimeric complex in cortical neurons. Wild-type CL3 tagged with either HA-tag (HA-CL3) or GFP (GFP-CL3) were coexpressed in cortical neurons by nucleofection and coimmunoprecipitated using an anti-GFP antibody. In, input; IP, immunoprecipitates.

inhibitor of squalene synthase that efficiently depletes membrane cholesterol (Figure 2B, lower panel). These results indicated that CL3 was a genuine component of dendritic lipid rafts and that raft insertion was likely regulated by CL3 prenylation and palmitoylation.

Does CL3 actually share some of the properties known for dendritic raft signaling molecules? A number of raft proteins were previously reported to homo-oligomerize into a multimeric protein complex via lipidification (Zacharias et al., 2002; Huang and El-Husseini, 2005). Indeed, HA-tagged WT CL3 coimmunoprecipitated with GFP-CL3 (Figure 2C) in cortical neurons. Furthermore, a significant fluorescence energy transfer (FRET) was detected between coexpressed CFP-CL3 and YFP-CL3 in live hippocampal neurons, indicative of their genuine molecular proximity in a complex (Figure S2A). Interestingly, Lyn, a well known raft-enriched molecule, colocalized with CL3 in live-untreated, but not in detergent-treated, neurons (Figure S2B). In contrast, the distribution of GluR1, a dendritic protein that is targeted to lipid rafts by palmitoylation (Suzuki et al., 2001; Hering et al. 2003; Hayashi et al. 2005), partially overlapped with CL3 even in detergent-treated neurons (Figure S2C).

CL3 Promotes Dendritogenesis in Cortical Neurons

From previous studies (Takemoto-Kimura et al., 2003; Wayman et al., 2004), it has been speculated that the CaMKK-CaMKI pathway might play a role in the control of neuronal morphology during development. In situ hybridization of embryonic day 17.5 (E17.5) tissues revealed a strong expression of CL3 transcript in the forebrain (Figures 3A and 3B) and in particular in the cortical plate of the cerebral cortex (Figures 3C and 3D). To test whether CL3 was involved in neuronal morphogenesis during this period, either GFP or GFP-CL3 cDNAs were

electroporated into cortical neurons immediately upon dissociation, and the morphology of the neurons was examined 48 hr later, a time point when the majority of neurons under our culture conditions developed well-discernable dendrites and one axon. In control GFP-expressing neurons, little GFP fluorescence overlapped with a Golgi membrane marker, GM130 (Figures 3E and 3F, arrow). In GFP-CL3-overexpressing cortical neurons, however, GFP fluorescence colocalized with GM130 (Figures 3G and 3H, arrow) and also showed discrete enrichment within several dendritic processes (Figures 3G and 3H, arrowhead). Compared to GFP-expressing control neurons (Figure 3I), GFP-CL3-overexpressing neurons appeared to exhibit unaltered axonal extension and branching, while in contrast, increased dendritic growth was found at and in the very vicinity of the soma (Figure 3L). In keeping with this finding, coexpression of mCherry-actin with GFP-CL3 (Figures 3M and 3N), but not with GFP (Figures 3J and 3K), revealed an augmentation of actin-enriched tips at the growing ends (Figures 3M and 3N, arrows) of the nascent processes extending out from the soma, consistent with activation of an actin cytoskeletal remodeling process. To quantify the morphological changes associated with CL3 overexpression, morphometric analyses were performed on the dendrites of GFP-CL3-expressing cortical neurons in a blind fashion. We found that total dendritic length, and in particular the length of the longest dendrite, was most strikingly increased by CL3 overexpression, while the change in branch-tip number remained small and not significant (Figure 3O). CL3-dependent promotion of dendritic growth was detected equally over the whole range of length of primary dendrites (Figure 3P), suggesting that the CL3 effect was unlikely to be restricted to just a subgroup of dendrites, but rather promoted a key common step in early dendritic formation. This CL3-induced effect was not seen with a kinase-inactive K52A mutant (data not shown). Together, these sets of evidence suggested the possibility that CL3 may be involved in early stages of dendritogenesis in developing cortical neurons.

A Required Role of CL3 in Dendritogenesis but Not in Axonogenesis

To critically test this possibility, we next examined the neuronal morphology in neurons where CL3 expression was strongly attenuated by RNA interference, using a short hairpin-type pSUPER vector that also coexpressed a PGK promoter-driven EGFP or mRFP1 gene cassette for morphological tracing. The knockdown efficiency and specificity of the shCL3 vector was prominent enough such that even an overexpressed GFP-CL3 became barely detectable 48 hr after transfection, while the control mRFP1 expression level remained unchanged (Figure 4A). This shCL3 vector was introduced into embryonic cortical neurons by electroporation, and formation of dendrites and axons was studied 48 hr later. While the cortical neurons showed 5–6 dendritic processes in control experiments, shCL3-treated neurons revealed a notable impairment in the number and total length of MAP2-positive dendrites (Figure 4B, arrows). In striking contrast, formation of Tau-1-positive axons was largely spared (Figure 4B, arrowheads). Quantitative morphometric analyses on dendritic or axonal arborizations confirmed that the impairment in shCL3-transfected neurons was actually confined to a selective decline in total dendritic length and in total tip number and did not affect either axonal outgrowth or branching (Figures 4C and 4D). The reduction in dendritic growth was observed throughout the whole range of dendrite length (Figure S3). The striking specificity in dendritic phenotype was also sustained even in shCL3-transfected neurons that were plated following an extensive period (48 hr) of suspension culture that allowed them to maximize the effect of knockdown prior to plating (Figure S4). Knockdown of either CaMKIIα or CaMKIV revealed no phenotype, at least during the very early dendritogenic period that we examined (Figure S5). Taken together, knockdown of CL3 did not interfere with the process of axon specification or axonogenesis, but rather suppressed a subsequent process that was required for dendritogenesis. We next asked whether CL3's kinase activation was a genuine requirement. The abnormality in dendritogenesis could be rescued by additional expression of an shCL3-resistant WT (kinase-active) CL3, but not by that of an shCL3-resistant K52A (kinase-inactive) CL3, demonstrating the absolute necessity of CL3 kinase activity during dendritogenesis (Figure 4E). Consistently, early dendritogenesis, but not axonogenesis, was also impaired in cultured cortical neurons obtained from CL3 null mice (Figure 4F).

In 9 DIV hippocampal neurons, CL3 knockdown diminished total dendritic length and primary dendrite number (Figure S6) and induced an altered Golgi morphology (Figure S7), which was somewhat reminiscent of Golgi vesiculation associated with impaired dendritic polarity (Horton et al., 2005).

A Required Role for CL3 in BDNF-Stimulated Dendritic Growth

We then asked what calcium mobilization might contribute to CL3-dependent stimulation of dendrite development. Brain-derived neurotrophic factor (BDNF) was previously shown to strongly promote dendrite growth and trigger an intracellular calcium rise (e.g., Huang and Reichardt, 2003, for a review). Consistent with published literature, bath application of BDNF induced a slow but clear increase in intracellular Ca^{2+} concentration in the cultured cortical neurons used in our study (Figures 5A–5C). Latencies of onset and oscillatory amplitudes/frequencies varied from neuron to neuron (Figures 5B and 5C). Continuous treatment of cortical neurons with BDNF significantly promoted dendritic growth (Figure 5D, $p < 0.05$, ANOVA with post hoc Tukey-Kramer test). In the presence of a global blocker of CaM kinase activation, KN-93, both constitutive and BDNF-stimulated components of dendritic growth were strongly inhibited

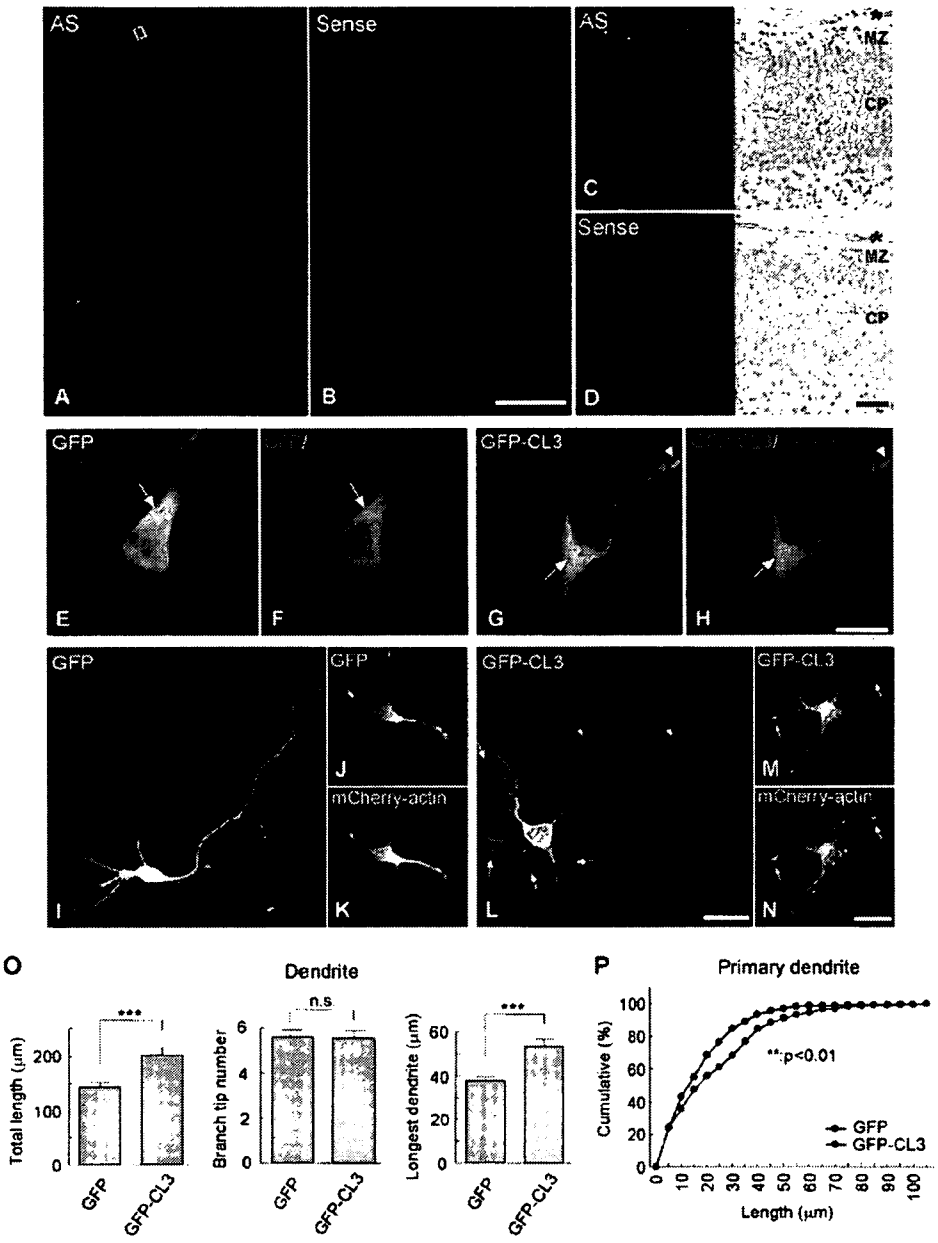

Figure 3. Expression of CL3 in the Developing Cortex and Regulation of Dendritic Morphogenesis in Cultured Cortical Neurons

(A–D) In situ hybridization of mouse embryonic (E17.5) tissue using an antisense (AS) riboprobe revealed an intense signal of CL3 transcript in the developing forebrain. The boxed area of a macroscopic image in (A) is shown at higher magnification (C): (left) hybridized DIG signal only; (right) full-color image (DIG signal in blue-violet + nuclear counterstaining in red). The control sense probe detected little signal (B and D). Asterisk, pia mater; MZ, marginal zone; CP, cortical plate.

(E–H) Membrane localization of CL3 in embryonic cortical cultures. GFP-CL3 distribution detected by anti-GFP immunostaining (G and H) showed colocalization with a Golgi marker, GM130 ([G and H], arrows). GFP-CL3 signals were also enriched within tips of fine dendritic processes ([G and H], arrowheads). Note that the GFP signals in control neurons were separated from the red GM130 immunofluorescence (E and F). Single representative confocal sections are shown.

(I–N) Overexpression of GFP-CL3 facilitated formation of actin-rich thin processes from dendrites and soma. Low-magnification image showed GFP-CL3 signals were distributed both in the nascent dendrites and in the axon ([L], arrow and arrowhead, respectively). In GFP-CL3-expressing neurons, a larger number of thin processes reminiscent of fine dendrites and/or filopodia were present at dendrites and soma ([L and M], arrows), as compared with GFP-expressing neurons (I and J), but not at the axon ([L], arrowheads). These numerous processes contained abundant amounts of β-actin, as shown by enrichment of mCherry-actin (arrows in [N]).

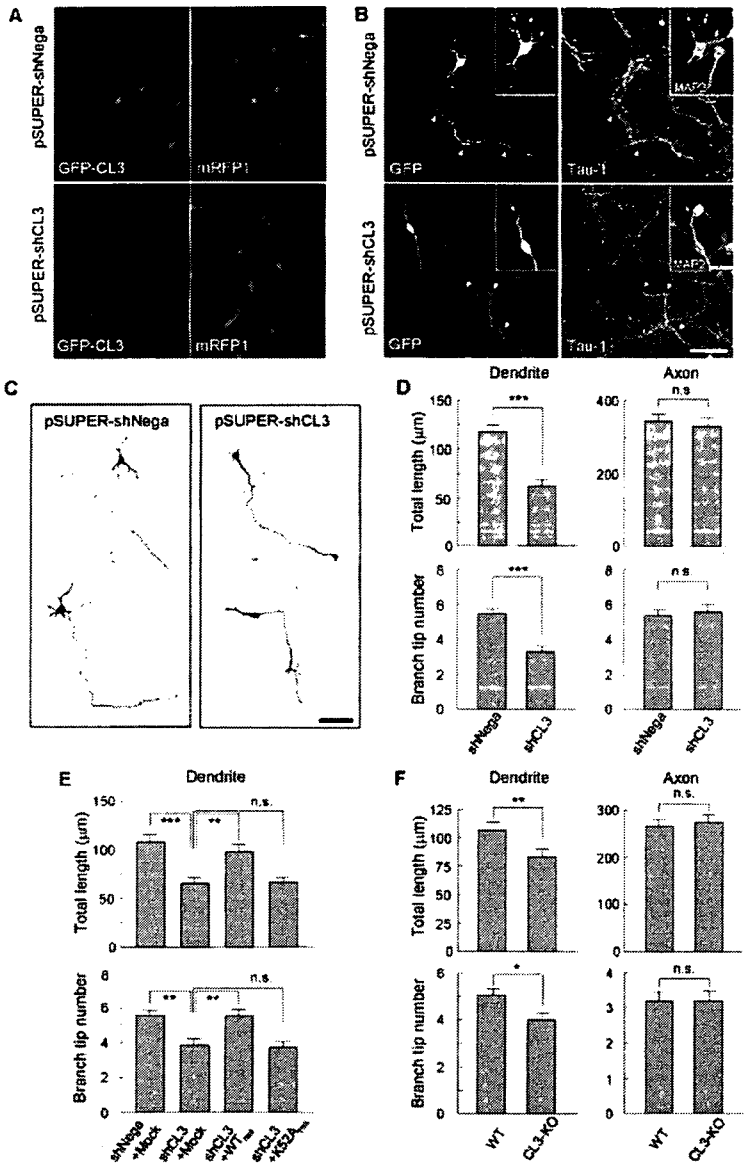

Figure 4. CL3 Loss-of-Function in Embryonic Cortical Neurons Elicits a Specific Impairment in Dendrite Morphogenesis

(A) Efficient downregulation of exogenous GFP-CL3 was achieved by a CL3-targeted shRNA vector (pSUPER-shCL3), but not by a control vector (pSUPER-shNega), in embryonic cortical neurons. The mRFP1 expression, which was driven by a dual promoter in a pSUPER + mRFP1 vector cassette, remained unchanged.

(B) A representative confocal image of an shCL3/GFP-expressing neuron (pSUPER-shCL3) showing impaired dendritogenesis. In this example, an shCL3-expressiong neuron had only a single remaining dendrite (an arrow in the inset), while an shNega-transfected neuron carried 5–6 dendrites (arrows in the inset). On the other hand, no change in axonal morphology was detected (arrowheads). Tau-1 and MAP2 were used to identify axons and dendrites, respectively.

(C) Monochrome diagrams of representative shNega- or shCL3-expressing neurons. The longest process (axon) was unchanged, while the morphology of shorter dendrites near the cell soma was much simplified in shCL3-transfected neurons.

(D) Quantification of morphometric parameters in CL3-knockdown neurons. To quantify, the total length and the dendritic branch tip number were calculated over the dendritic or the axonal arborizations for all branches exceeding 7 μm in length. In shCL3-expressing neurons, both parameters were significantly reduced in the dendrites. On the other hand, neither axonal length nor axonal branch tip number were significantly altered. Number of neurons: shNega, n = 78; shCL3, n = 53. ***p < 0.001; n.s., not significant (p > 0.05) (t test).

(E) Requirement for CL3 kinase activity to rescue shCL3-mediated impairment in dendritogenesis. Introduction of an shCL3-resistant silent mutant of wild-type GFP-CL3 (WT_{res}) successfully rescued the dendritic phenotype elicited by shCL3 on both morphometric parameters. The shCL3-resistant kinase-inactive GFP-CL3 ($K52A_{res}$) was unable to rescue the shCL3 phenotype. Number of neurons: shNega, n = 37; shCL3 + mock, n = 35; shCL3 + WT_{res}, n = 41; shCL3 + $K52A_{res}$, n = 33. **p < 0.01; ***p < 0.001; n.s., not significant (p > 0.05) (ANOVA with post hoc Tukey-Kramer test).

(F) Dendritogenesis, but not axonogenesis, is specifically impaired in cultured cortical neurons from CL3-KO mice. WT, n = 20; CL3-KO, n = 20. *p < 0.05; **p < 0.01; n.s., not significant (p > 0.05) (t test). Scale bars, 50 μm (A–C) and 20 μm ([B], inset).

(Figure 5D). Because KN-93 suppressed dendritic growth to a similar extent under either constitutive or BDNF-stimulated conditions, this raised the possibility of a common involvement of a KN-93-sensitive kinase (Figure 5D). To specifically test this idea, we employed RNAi and measured the degree of suppression of dendritic growth in the absence or presence of BDNF application and found that indeed CL3 knockdown completely phenocopied the effect of KN-93 on dendrites and occluded BDNF-stimulated dendritic growth (Figure 5E).

(O) Facilitation of dendritic outgrowth by CL3 overexpression. Total length, branch tip number, and longest dendrite length are shown. Number of neurons: GFP, n = 30; GFP-CL3, n = 30. ***p < 0.001; n.s., not significant (p > 0.05) (t test).

(P) Cumulative probability analysis shows a significant extension of primary dendrites in GFP-CL3-expressing neurons (**p < 0.01, Kolmogorov-Smirnov test). Numbers of examined dendrites: GFP, n = 258 (from 50 neurons); GFP-CL3, n = 321 (from 50 neurons).

Scale bars, 300 μm (A and B); 50 μm (C and D); 10 μm (E–H); 20 μm (I–N).

Furthermore, dendritic growth was rescued by coexpressing an shCL3-resistant wild-type, but not a membrane anchoring-defective CL3 mutant (Figure 5F). Thus, signaling via membrane-anchored CL3 may play a critical role in BDNF-mediated cortical dendritogenesis during early development.

A Lipid-Raft-Delineated CL3-STEF-Rac Pathway Contributes to the Development of Cortical Dendrites

What are the signaling components that underlie lipidified CL3-mediated dendritic growth? Taking advantage of our finding that CL3 overexpression was accompanied by a sizable increase in the length of primary dendrites (Figures 3O, 3P, and 6A), and in particular its longest dendrite (Figure 3O, right panel; Figure 6B), we next tested the possible contribution of small GTPases downstream of CL3. Coexpression of a dominant-negative Rac abolished the effect of CL3 overexpression (Figures 6A and 6B), and this effect was seen throughout the observed range of primary dendrite length (Figure 6C), supporting the idea that Rac mediated CL3-stimulated dendritic growth. Consistently, we found that CL3 knockdown downregulated Rac activity (Figure 6D). Furthermore, overexpression of a dominant interfering fragment (PHnTSS) of STEF, a specific RacGEF previously implicated in cortical migration and neurite outgrowth (Kawauchi et al., 2003; Matsuo et al., 2002), also potently repressed the CL3 effect (Figures 6A and 6B); however, this effect was less pronounced in dendrites with shorter lengths (<20 μm) (Figure 6C). Both STEF and Rac were detected in the Triton X-100-insoluble low-density membrane fractions enriched for flotillin-1 but devoid of transferrin receptors (Figure 6E), consistent with the presence of a raft-delineated CL3-STEF-Rac pathway. In keeping with this, sustained Rac activity significantly attenuated the impairment in dendrite development observed in CL3-diminished neurons (Figures 6F and 6G).

If raft localization of CL3 was critical for CL3-dependent dendritogenesis, a raft depletion by pharmacological manipulation or a removal of CL3 from rafts by mutation of its palmitoylation sites should significantly perturb dendrite formation and growth. To test this, we pretreated cortical neurons with either mevastatin, an HMG-CoA reductase inhibitor, to deplete membrane cholesterol, and/or with fumonisin B_1, an inhibitor of sphingolipid synthesis. Treatment with either mevastatin or, to a lesser extent, with fumonisin B_1 reduced dendritogenesis (Figures 7A and 7B). A combination of both had no further additive effect (Figures 7A and 7B). As mevastatin was expected to interfere not only with cholesterol synthesis alone but also with protein prenylation, we also examined the effect of zaragozic acid, an inhibitor of squalene synthase, which would disrupt cholesterol synthesis while sparing mevalonate production. Zaragozic acid treatment diminished dendrite formation to a degree similar to the effect seen with mevastatin; a combination of both did not produce a further incremental effect (Figures 7A and 7B). Interestingly, raft depletion by treatment with zaragozic acid abolished the dendritogenic action of overexpressed CL3 (Figure 7C). Together, these results further supported the idea that the presence of intact lipid rafts was critical for CL3 to exhibit its dendritic effect.

In keeping with this, a palmitoylation-site-deficient 4CS mutant of CL3, which was made resistant to shCL3 RNAi vector, was unable to rescue the dendritic effect of CL3 knockdown in cortical neurons (Figure S4C). Intriguingly, in hippocampal neurons, the inaccessibility of 4CS mutant protein toward detergent-resistant raft membranes in CL3-knockdown cells (Figure S8A) was accompanied with the appearance of exuberant thin filopodial processes from the soma (Figure S8B, arrows). These results are consistent with a role of palmitoylation in targeting, and perhaps restricting, CL3 expression to its appropriate sites of cellular actions. Taken together, CL3 palmitoylation may be a useful means to restrict STEF-Rac activation to microdomains in the vicinity of dendritic rafts during early dendritogenesis.

DISCUSSION

Identification of CL3/CaMKIγ as a Privileged Kinase Involved in the Regulation of Dendritic Cytoarchitecture during Early CNS Development

Previous analyses have established the necessity of CaMKII, a predominant form of CaM kinase, as molecular switch required for neuroplasticity in the hippocampus, the barrel cortex, and the visual cortex (Lisman et al., 2002; Fox and Wong, 2005). Furthermore, the role of CaMKII isoforms in several forms of dendritic development was extensively studied, though the exact effect on dendrite morphogenesis has remained rather controversial. CaMKIIα was shown to contribute to dendritic outgrowth in cerebellar granule neurons (Gaudilliere et al., 2004), and CaMKIIβ but not CaMKIIα regulated the movement and branching of filopodia and fine dendrites in rat hippocampal neurons (Fink et al., 2003). In contrast, in *Xenopus* retinotectal neurons, CaMKII was reported to limit dendritic outgrowth and to stabilize dendritic arborization in vivo (Wu and Cline, 1998).

In contrast to CaMKII, which is one of most abundant proteins expressed in the postsynaptic density (PSD) (Kennedy, 2000), CaMKIV in the nucleus plays a critical role in mediating Ca^{2+}-regulated transcription via a CREB/CBP pathway, which is necessary for the formation of long-term synaptic plasticity and long-term memory (Silva et al., 1998; Bito and Takemoto-Kimura, 2003), as well as activity-dependent dendritic elongation (Redmond et al., 2002). In turn, a cytosolic CaMKI activity has been shown to participate in the gating of an ERK/MAP-kinase-dependent form of LTP (Schmitt et al., 2005). Neurite outgrowth was also reported to be regulated by a presumably cytosolic CaMKK-CaMKI/IV pathway: indeed, a constitutively active CaMKIV was suggested to enhance dendritic growth via stabilization of β-catenin (Yu and Malenka, 2003), while a CaMKK inhibitory drug, STO-609, or putative dominant-negative constructs specifically blocking

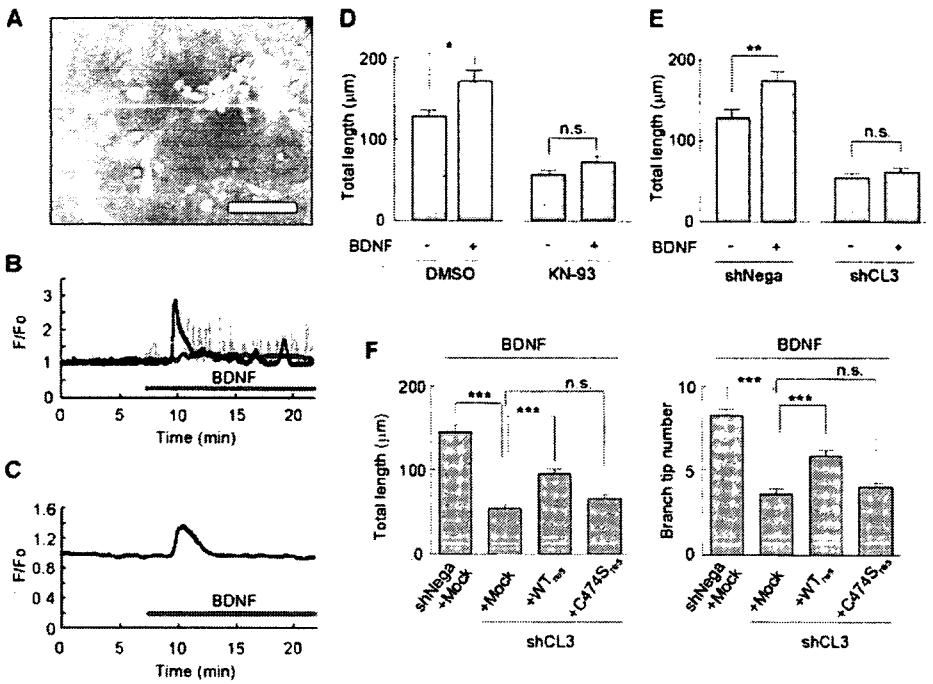

Figure 5. Requirement of CL3 for BDNF-Stimulated Dendrititogenesis

(A) BDNF-induced calcium transients in developing cultured neurons. A representative image of cortical neurons during a typical calcium rise after BDNF bath application is shown in (A). Embryonic cortical neurons (1 DIV) were loaded with a calcium indicator, Fluo-4AM, and calcium responses were measured by time-lapse imaging. A green fluorescence image was overlaid on a DIC image. Colored boxes indicate the location of cells shown in (B). Scale bar, 50 μm.

(B) Representative calcium responses in individual cells after BDNF administration. Three different types of calcium responses were revealed. The majority of cells showed a large transient response followed by smaller repetitive responses (blue), whereas some showed oscillation (yellow) or chronic increases from the baseline (red).

(C) Averaged calcium responses after BDNF administration. An averaged response from 70 cells in a microscopic field is shown.

(D) Cortical neurons were transfected with a morphological tracer, mCherry, and stimulated with BDNF from 6 hr to 48 hr after plating, in the presence or absence of KN-93, a general CaM kinase inhibitor. BDNF treatment maximized dendritogenesis, and this BDNF-stimulated increment was occluded in neurons treated with KN-93. Numbers of neurons: vehicle + DMSO, n = 25; vehicle + KN-93, n = 44; BDNF + DMSO, n = 38; BDNF + KN-93, n = 32.

(E) Quantification of dendritogenesis in BDNF-stimulated CL3-knockdown neurons. CL3 knockdown severely inhibited dendritogenesis induced by BDNF administration, to an extent similar to that obtained with KN-93. Numbers of neurons: vehicle + shNega, n = 40; vehicle + shCL3, n = 41; BDNF + shNega, n = 40; BDNF + shCL3, n = 40.

(F) Suppression by CL3 knockdown of BDNF-stimulated dendritogenesis can be rescued by coexpression of an shRNA-resistant wild-type CL3 (WTres), but not by a nonlipidified mutant CL3 (C474Sres). Numbers of neurons: shNega + mock, n = 52; shCL3 + mock, n = 57; shCL3 + WTres, n = 57; shCL3 + C474Sres, n = 55.

***p < 0.001; n.s., not significant (ANOVA with post hoc Tukey-Kramer test).

either CaMKK or cytosolic CaMKI/CaMKIV (but not nuclear CaMKIV) activities prevented axonal extension and growth cone dynamics as well as neurite extension (Schmitt et al., 2004; Wayman et al., 2004).

Taken together, multiple CaM kinase pathways that are segregated in distinct subcellular compartments may regulate several critical steps converging onto dendrite elongation and maturation. This prompted us to investigate the particular role of CL3/CaMKIγ (Takemoto-Kimura et al., 2003; Nishimura et al., 2003), a membrane-anchored form of CaMKI, which was highly expressed in the cortical plate neurons of the mouse embryo (this study). Intriguingly, we found a specific impairment in the number and total lengths of dendrites in CL3 knockdown and CL3 null neurons (Figure 4 and Figure S3), while axonal morphology was not significantly distinct from controls. Knockdown of CL3 prior to plating of neurons strengthened this suppressive effect on the dendrites while still sparing the axons (Figure S4). Taken together, our data suggested a prominent role of CL3 during the early stages of dendritogenesis that presumably followed completion of the axon/dendrite specification.

While this paper was under review, an independent study reported that CL3/CaMKIγ may regulate activity-dependent dendritic growth at an even later stage of development in hippocampal neurons (Wayman et al., 2006; see also Figures S6 and S7 of this study).

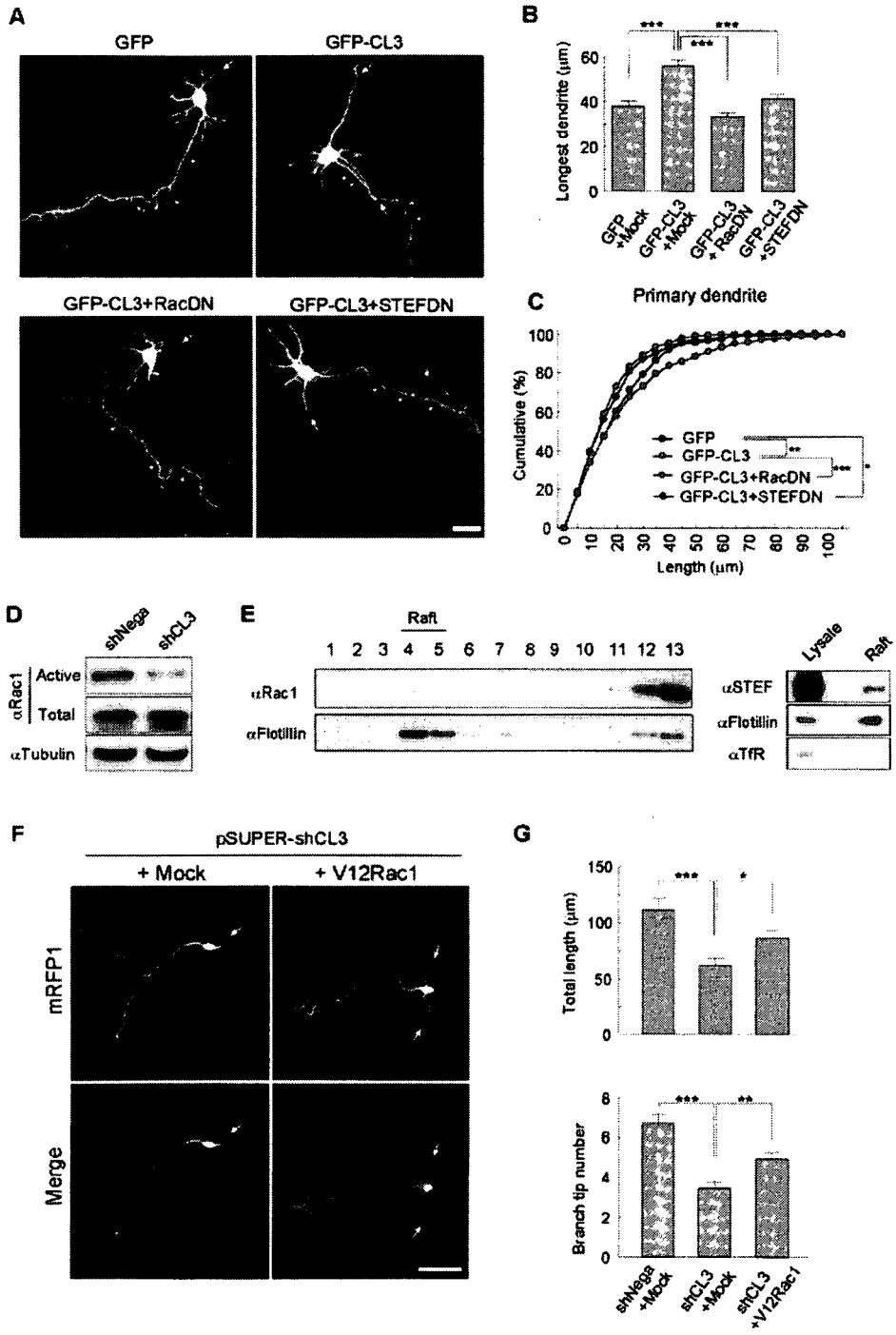

Figure 6. A Critical Role for RacGEF STEF and Rac in Mediating CL3-Induced Dendritic Outgrowth

(A) Cortical neurons were cotransfected with GFP-CL3 and either dominant-negative Rac1 (RacDN) or dominant-interfering fragment of STEF (STEFDN) together with a morphometric tracer, mRFP1. Examples for dendrites (arrows) and axons (arrowheads) are shown. Scale bar, 20 μm.

(B) Quantification of longest dendrite. Number of neurons: GFP + mock, n = 51; GFP-CL3 + mock, n = 50; GFP-CL3 + RacDN, n = 57; GFP-CL3 + STEFDN, n = 60. ***$p < 0.001$ (ANOVA with post hoc Tukey-Kramer test).

(C) Cumulative probability analysis of the length of primary dendrites showed that inhibition of STEF and Rac activity suppressed the extension of primary dendrites induced in GFP-CL3-expressing neurons. Number of examined dendrites (neurons): GFP, n = 324 (from 51 neurons); GFP-CL3, n = 332 (from 50 neurons); GFP-CL3 + RacDN, n = 328 (from 57 neurons); GFP-CL3 + STEFDN, n = 378 (from 60 neurons). *$p < 0.05$; **$p < 0.01$; ***$p < 0.001$ (Kolmogorov-Smirnov test).

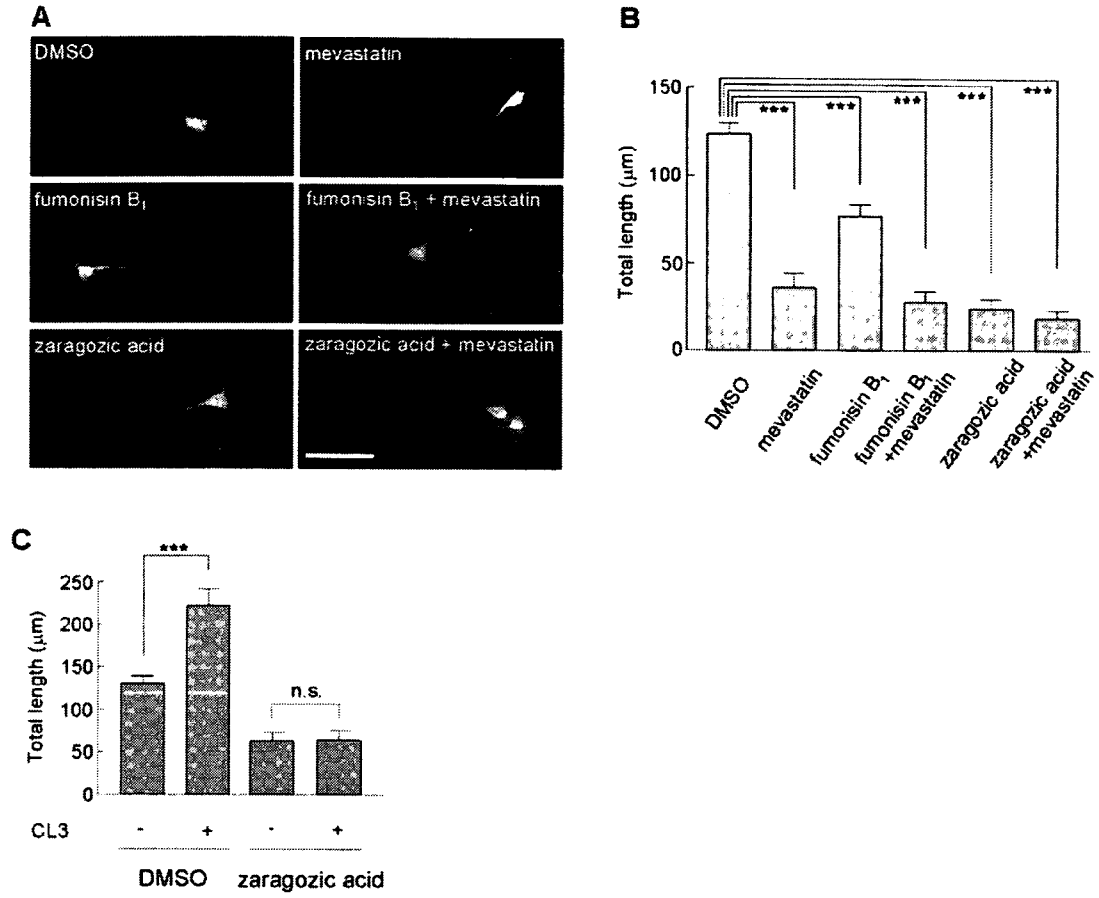

Figure 7. Raft Depletion Abolishes CL3-Mediated Dendrite Outgrowth

(A) Cortical neurons were transfected with a morphological tracer, mCherry, and cultured in the presence of various combinations of raft-depleting agents from 6 hr to 48 hr after plating. Disruption of cholesterol/sphingolipid synthesis strongly inhibited formation and outgrowth of the dendritic processes around the soma. Scale bar, 50 μm.

(B) Ensemble average of experiments shown in (A). DMSO, n = 10; 10 μM mevastatin, n = 15; 10 μM fumonisin B_1, n = 15; 10 μM fumonisin B_1 and 10 μM mevastatin, n = 15; 100 μM zaragozic acid, n = 15; 100 μM zaragozic acid and 10 μM mevastatin, n = 15. ***p < 0.001 (ANOVA with post hoc Tukey-Kramer test).

(C) Raft depletion using zaragozic acid abolished the increase of dendritogenesis induced by CL3 overexpression. A significant CL3-mediated increase in dendritic growth was shown in the DMSO control, but this significant increase was abolished by raft depletion in the presence of zaragozic acid (two-way ANOVA, CL3 effect, $F_{1,65} = 8.65$, $p = 0.0045$; drug effect, $F_{1,65} = 51.95$, $p < 0.0001$; CL3 × drug, $F_{1,65} = 8.38$, $p = 0.0052$). ***p < 0.001 (post hoc Bonferroni test). DMSO, n = 15 (−CL3), n = 24 (+CL3), 100 μM zaragozic acid, n = 15 (−CL3), n = 15 (+CL3).

Control of CL3 Targeting to Lipid Microdomains by a Kinase-Activity-Regulated Dual Lipidification Mechanism

In polarized neural cells, covalently attached lipid modification of proteins is important for membrane targeting and expression of proper function in the vicinity of specialized membrane compartments. Largely based on quantitative work on Ras and PSD-95, a palmitoylation/depalmitoylation cycle has been previously suggested to play a crucial regulatory role in determining the proper

(D) The amount of GTP-bound active Rac1 was measured by a Pak1-PBD pulldown assay using cortical neurons transfected with shNega or shCL3 vector. The amount of active Rac1 was reduced by CL3 knockdown.

(E) Presence of Rac1 and STEF immunoreactivities in lipid raft fractions of cortical neurons. For STEF detection, a pooled and concentrated raft fraction was used. Transferrin receptor was used as a non-raft membrane marker.

(F) Representative images of shCL3/mRFP1-expressing neurons coexpressing constitutively active GFP-Rac1 (+V12Rac1) or GFP (+mock). Expression of constitutively-active GFP-Rac1 (+V12Rac1) restored appearance of multiple dendrites (arrows) in shCL3-expressing neurons, while expression of GFP alone did not. Scale bar, 50 μm.

(G) Quantification of dendritic morphogenesis confirmed that constitutively active GFP-Rac1 attenuated the specific impairment of dendritic morphology induced by shCL3 transfection. Number of neurons: shNega + mock, n = 22; shCL3 + mock, n = 47; shCL3 + V12Rac1, n = 49. *p < 0.05; **p < 0.01; ***p < 0.001 (ANOVA with post hoc Tukey-Kramer test).

trafficking and function of palmitoylated signaling proteins (Huang and El-Husseini, 2005). Dynamic regulation of palmitoylation was already shown for a large number of synaptic constituents such as AMPA-receptor subunits (Hayashi et al., 2005), GABAR γ-subunits (Keller et al., 2004), and GRIP/ABP (DeSouza et al., 2002), indicating a critical role for neuronal PAT in synaptic maturation and maintenance. However, a direct involvement of protein palmitoylation in early stages of neuronal morphogenesis has not been examined.

In this work, we demonstrated that the C-terminal end of CL3 was covalently modified in a sequential manner by prenylation and by palmitoylation. A dually lipidified CL3 was generated in a kinase-activity-dependent manner, in part via the PAT GODZ (Uemura et al., 2002), resulting in an efficient enrichment into dendritic-raft-like lipid microdomains.

We then found that dually lipidified CL3 was likely to be partitioned and targeted to close proximity of dendritic lipid microdomains. Consistently, CL3 showed self-association (Figure 2C and Figure S2A), a property that is not unusual for palmitoylated or dually lipidified proteins (Zacharias et al., 2002). However, we failed to detect any Ca^{2+}/CaM-independent kinase activity of CL3, even under conditions where CL3 multimerization was present. This is distinct from the property of CaMKII, in which dodecamerization was shown to promote a Ca^{2+}/CaM-independent kinase activity that outlasted the duration of the incoming Ca^{2+} mobilization through an autophosphorylation mechanism. We thus speculate that oligomerization, if any, of prenyl-/palmitoyl-CL3 may have roles other than the generation of an autonomous kinase activity, such as sustaining a high degree of molecular proximity and concentration that favors signal amplification and increases the specificity and efficiency of coupling to downstream signaling events.

A BDNF-CL3-Rac Pathway May Underlie Excitation-Morphogenesis Coupling during Early Cortical Dendritogenesis

Previously, neuronal activity has been shown to promote initiation of dendrite formation via small GTPases such as Rac and Cdc42 (Luo, 2002; Van Aelst and Cline, 2004). To date, however, knowledge about how neuronal activity regulates these small GTPases is still limited. The strongest evidence in favor of activity-induced dendritic arborization so far involved several Ca^{2+}-regulated transcriptional factor such as CREB, NeuroD, and CREST (Gaudilliere et al., 2004; Konur and Ghosh, 2005), though the cellular mechanisms linking nuclear events and neuronal morphogenesis remained as yet largely undetermined. Here we found that a membrane-bound CaM kinase, CL3/CaMKIγ, may possibly act downstream of BDNF and Ca^{2+} signals to promote dendritic cytoskeletal remodeling via the small GTPase Rac, especially during early stages of dendritic development. Furthermore, we provided several lines of evidence that collectively indicated that CL3-STEF-Rac signaling triggered at or in the vicinity of lipid rafts may play a critical role.

Could lipid rafts, also known as sphingolipid- and cholesterol-rich membrane microdomains, be distributed in an asymmetric fashion such that some of these may influence dendrite targeting of signaling proteins such as CL3? In support for such an idea, depletion of cellular cholesterol/sphingolipid content in cultured neurons revealed an important role for cholesterol (Fan et al., 2002) or sphingolipids (Schwarz and Futerman, 1998; Pelled et al., 2003) in dendritic growth and spine maintenance (Hering et al., 2003). In addition, no responsiveness to glutamate application was reported in neonatal cortical neurons of a mutant mouse deficient in cholesterol biosynthesis, despite a normal amount of GluR and NMDAR subunit expression, indicating a possible defect in membrane insertion of dendritic glutamate receptors (Wassif et al., 2001). A distinct kind of raft-mediated asymmetry may play a role in axonal fate specification (Da Silva et al., 2005).

If raft formation was coupled with the creation of a polarized asymmetry of signaling molecule distribution, how could this possibly underlie a morphogenetic response, especially downstream of BDNF? Recruitment of activated TrkB to lipid rafts (Suzuki et al., 2004) could evidently contribute to efficient coupling to raft-targeted CL3 downstream of BDNF. In neurons, fractionation experiments during development have also previously revealed a privileged association of Rac with rafts, but not of RhoA or Cdc42 (Kumanogoh et al., 2001; see also Figure 6E). We additionally found that a portion of STEF was clearly present in the raft fractions as well (Figure 6E). As the fragment encompassing the PHnTSS domain of STEF (PHnTSS) has been shown to act as a specific dominant-negative form for both STEF and Tiam1 (Matsuo et al., 2002), it remains possible that there may also be an additional contribution of Tiam1, a known substrate for CaMK activity (Tolias et al., 2005).

Taken together, dual lipidification of CL3 may be an efficient mechanism not only to target it into rafts and to limit its protein diffusion parallel to the lipid bilayer, but also to generate a membrane-delimited area of Rac activation within segregated dendritic lipid microdomains at the vicinity of Ca^{2+}-mobilization events. Further studies are needed to substantiate such a hypothesis.

In conclusion, we here uncovered a novel role for CL3/CaMKIγ in the regulation of Rac-dependent dendritic cytoskeletal reorganization, and we found evidence for CL3 in mediating BDNF-stimulated dendritic growth. Through a dual and sequential lipidification mechanism, the unique C-terminal region of CL3 was covalently lipid-modified in a kinase-activity-dependent manner, leading to a privileged partition of membrane-anchored CL3 into dendritic-raft-like lipid microdomains. This membrane-sorting mechanism, unprecedented for a neuronal Ser/Thr kinase, in turn may efficiently localize Rac activity and thereby regulate dendritogenesis. Thus, CL3 turned